CHAPTER IV
RESULTS AND DISCUSSION

In this research, the effects of molecular weight difference of LDPE on mechanical properties and physical properties of LDPE/PLA blending were studied. Two grades of LDPE with different average molecular weight indices of 125 kg/mole and 240 kg/mole and compatibilizer from LLDPE-*g*-MA were used.

4.1 Rheological properties of LDPE/PLA blends

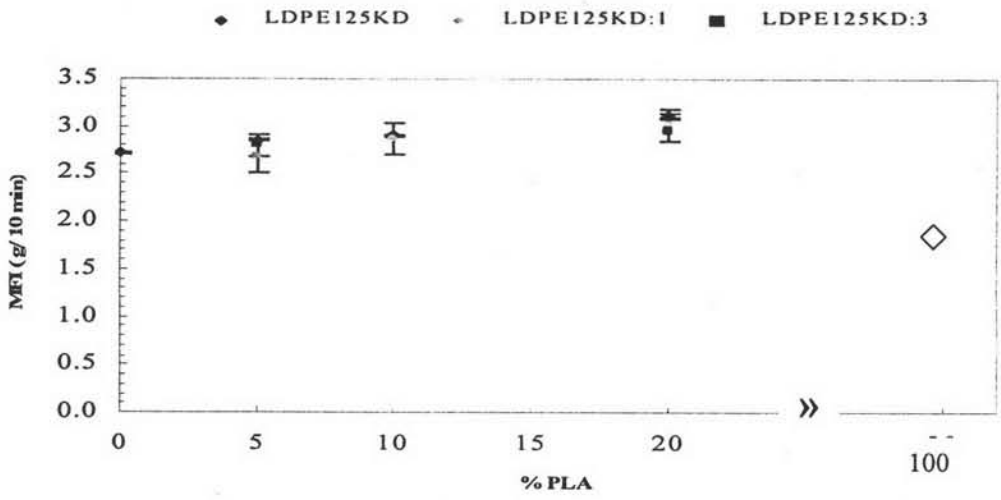

Figure 4.1 Melt flow indice of LDPE125KD/PLA blends and virgin polymers

The effects of blend ratio on MFI of the uncompatibilized and compatibilized of LDPE125KD/PLA and LDPE240KD/PLA blends are shown in Fig. 4.1- 4.2. Average MFI of PLA is obtained at 1.85 g/10 min. It was found that the melt flow index (MFI) of LDPE125KD/PLA blends increased with increasing PLA content compared with its virgins LDPE. This might be influenced by the incompatibility between two phases. Similar result was observed in LDPE240KD/PLA blends. The effect of compatibilizer was observed in very small in both of LDPE240KD/PLA and LDPE125KD/PLA (Fig. 4.1 -4.2) that MFI measurement cannot use for investigation in this study.

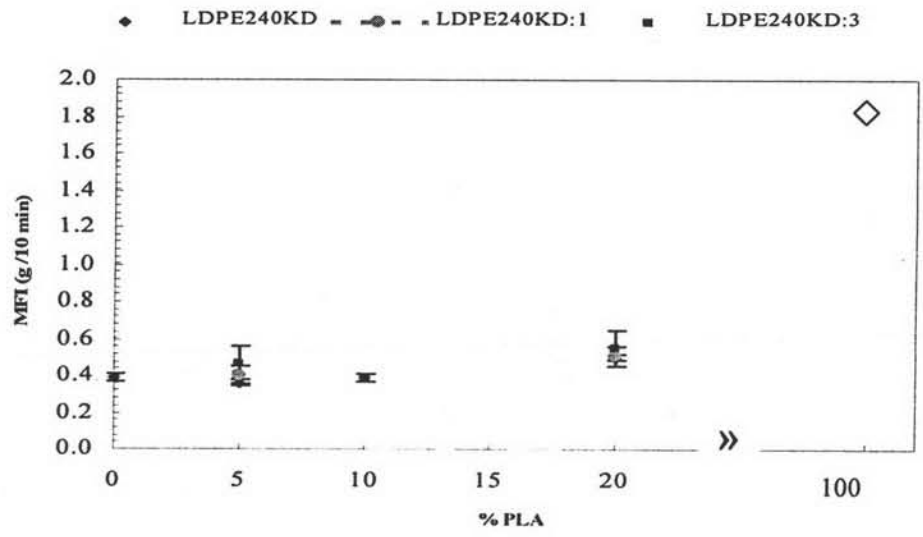

Figure 4.2 Melt flow indice of LDPE240KD/PLA blends and virgin polymers

4.2 Morphology of LDPE240KD/PLA and LDPE125KD/PLA blends at various PLA contents

4.2.1 Effect of PLA content

Because of the inherent incompatibility between polyolefin (LDPE) and polyester (PLA) between LDPE and PLA, their blends produ hase materials, indicating immiscibility of the blend components which both of virgin of LDPE's morphology and all uncompatibilized blends are showed in Figure 4.3. The blend volume ratio plays a predominant role in determining which of the two components form the dispersed phase and the matrix phase. Based on the blend volume, it indicates that, in the LDPE-rich blend, PLA forms the dispersed phase in the LDPE matrix. The scanning electron microscopy is employed to investigate the fractured surface of the specimen. Blending of LDPE125KD and LDPE240KD with PLA was composed of the two phased dispersions, including the matrix phase and dispersed phase as shown in Figure 4.3. There exists a sharp interface between the dispersed PLA and LDPE matrix. Dispersed PLA in LDPE240KD/PLA blends had spherical shape and better size distributions in LDPE240KD/80, especially comparison to the

results seen in Figure 4.3C and 4.3D. The size was increased when PLA content increased in LDPE240KD matrix as present in Figure 4.3G, 4.3E and 4.3C respectively. The dispersed PLA in LDPE125KD/PLA blends shows an elongated shape and a very broad size distribution in LDPE125KD/80(Figure 4.3D) which might be easier formed by coalescence from the amount of PLA than did LDPE240KD/80 that has larger molecular chains. The size of the dispersed phase in LDPE125KD/PLA blends is also larger when the amount of PLA increased (Figure4.3H, 4.3F and 4.3D). Moreover, there are voids from which the dispersed PLA was pulled out. They are abundantly presented and clearly observed in Figure 4.3. This is a typical morphology of an incompatible blend.

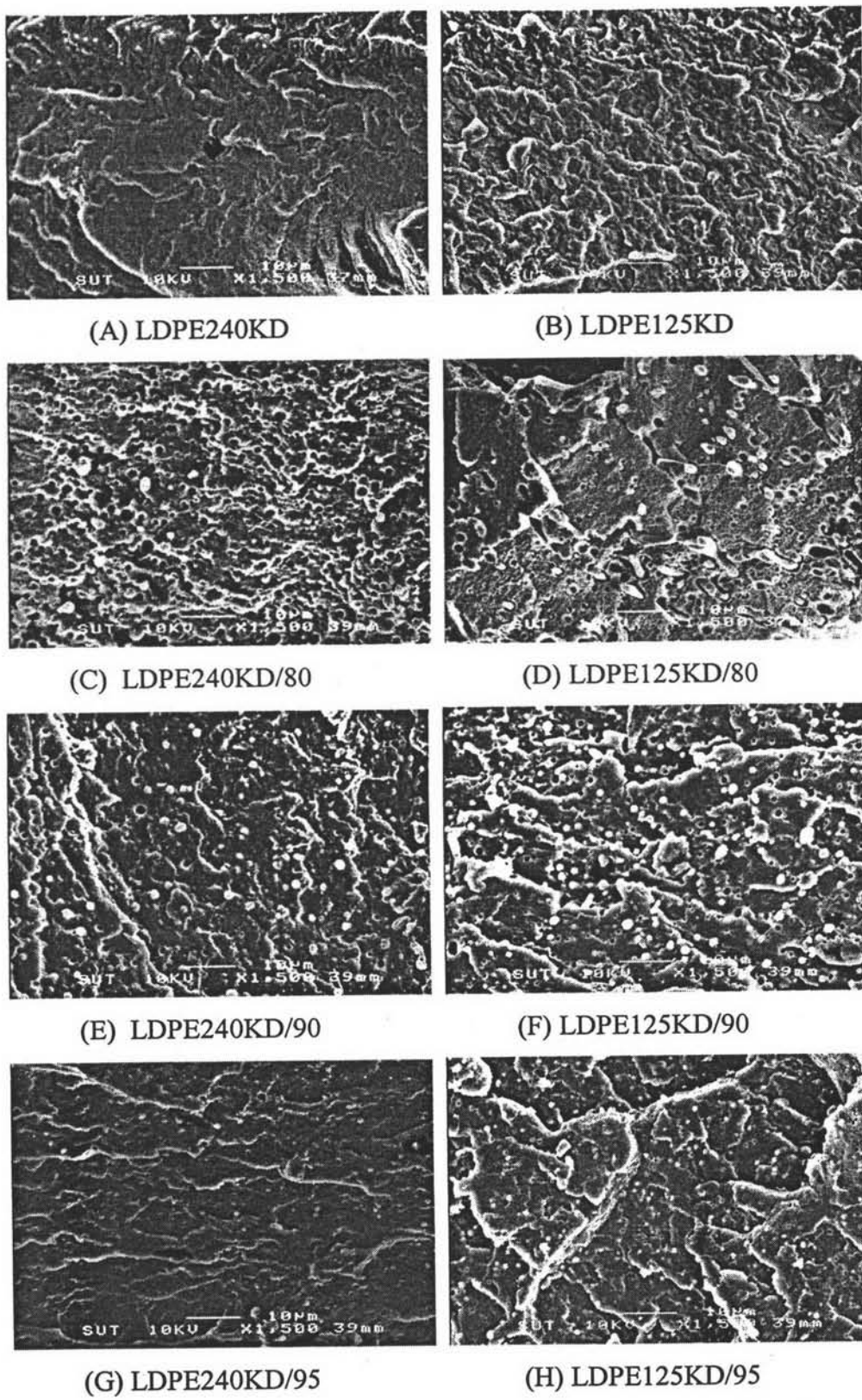

(A) LDPE240KD (B) LDPE125KD

(C) LDPE240KD/80 (D) LDPE125KD/80

(E) LDPE240KD/90 (F) LDPE125KD/90

(G) LDPE240KD/95 (H) LDPE125KD/95

Figure 4.3 Scanning electron micrographs showing the fractured surfaces of the uncompatibilized LDPE125KD/PLA and LDPE240KD/PLA: (A) LDPE240KD;(B) LDPE125KD;(C) LDPE240KD/80;(D) LDPE125KD/80;(E) LDPE240KD/90;(F) LDPE125KD/90;(G) LDPE240KD/95;(H) LDPE125KD/95

4.2.2 Effect of compatibilizer

The morphologies of compatibilized and uncompatibilized blends LDPE125KD/PLA and LDPE240KD/PLA with LLDPE-*g*-MA as the compatibilizer are shown in Figures 4.4 - 4.5. After the addition of 1 pphr of LLDPE-*g*-MA, the blends of LDPE240KD show finer and smaller particles of PLA scattering in the matrix as seen in Figure 4.4B.Whereas the blends of LDPE125KD illustrate that the shape dispersed phases of PLA were changed from elongated to spherical shape (Figure 4.5B and Appendix A) and lighter boundary was observed at interface. Additionally, Figure4.4D is also seen that adhesion increases between the dispersed and matrix phases in which the interface boundary is less observed especially in LDPE240KD/80:10 than LDPE240KD/80, LDPE240KD/80:1 and LDPE240KD/80:3 (Figure4.4A-4.4C). The reducing voids at the fractured surface are observed and obviously showed in LDPE240KD/80:10 (Fig. 4.4D) because an increasing amount of maleic anhydride did much more coupling the PLA chains onto LDPE chains.

All these results indicate that the role of LLDPE-*g*-MA concerns the stabilization of the blend morphology. These results further indicate that the presence of LLDPE-*g*-MA reduces interfacial tension in LDPE125KD/PLA interface more than in LDPE240KD. It is supported by reason that LLDPE block copolymer has higher adhesion value in that of polylactide and PE than HDPE block copolymer because of higher stiffness of HDPE [21].

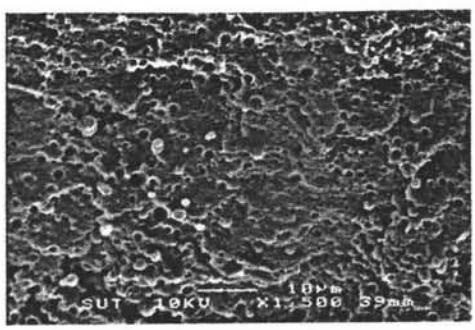

(A) LDPE240KD/80

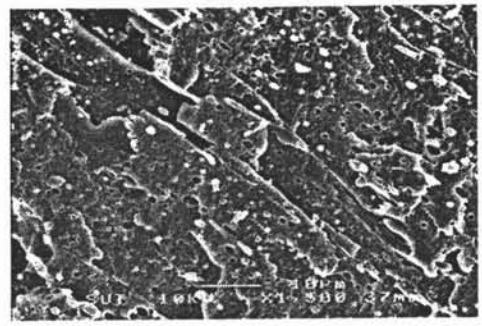

(B) LDPE240KD/80:1

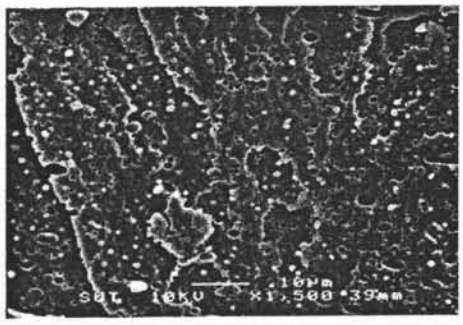

(C) LDPE240KD/80:3

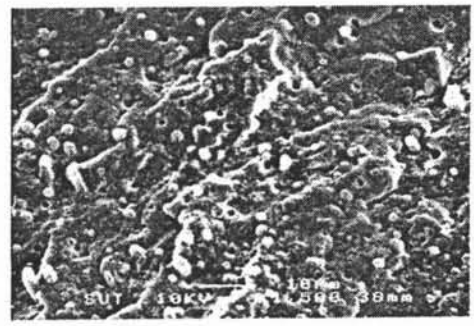

(D) LDPE240KD/80:10

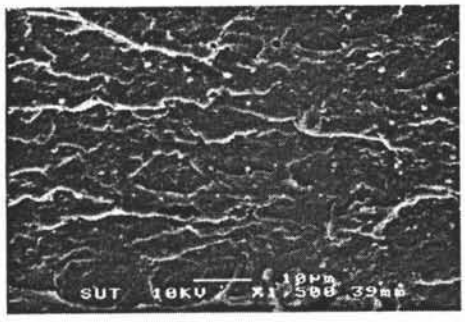

(E) LDPE240KD/95

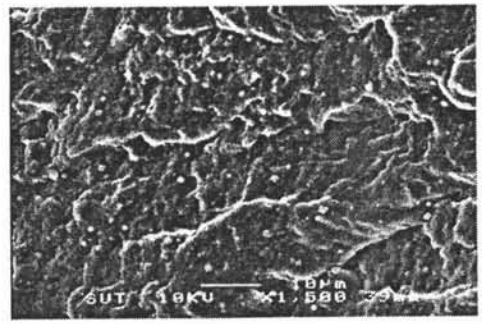

(F) LDPE240KD/95:1

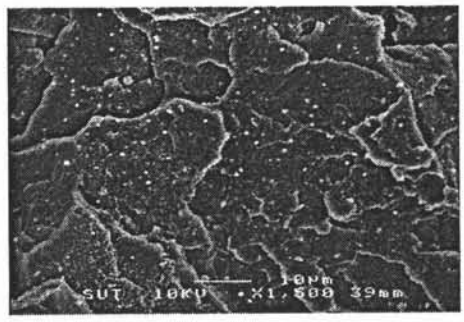

(I) LDPE240KD/95:3

Figure 4.4 Scanning electron micrographs showing the fractured surfaces difference between the uncompatibilized and the compatibilized LDPE240KD/PLA blends by LLDPE-*g*-MA compatibilizer: (A) LDPE240KD/80; (B) LDPE240KD/80:1; (C) LDPE240KD/80:3; (D) LDPE240KD/80:10; (E) LDPE240KD/95; (F) LDPE240KD/95:1; (I) LDPE240KD/95:3

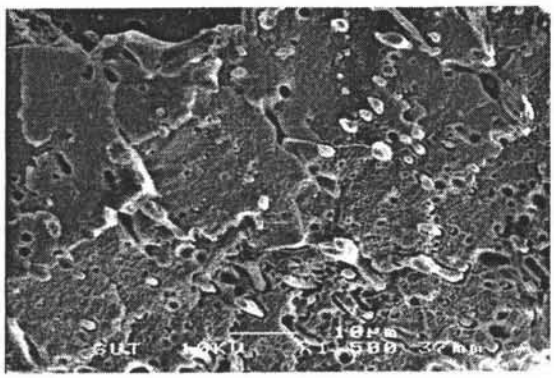

(A) LDPE125KD/80

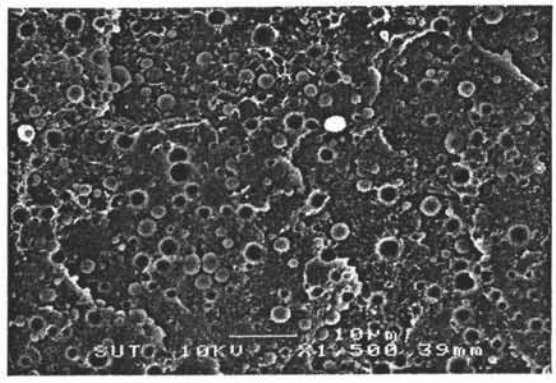

(B) LDPE125KD/80:1

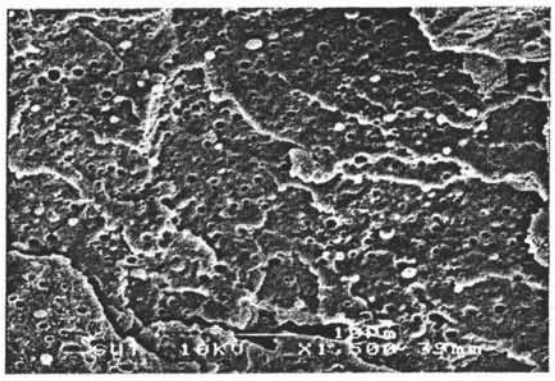

(C) LDPE125KD/80:3

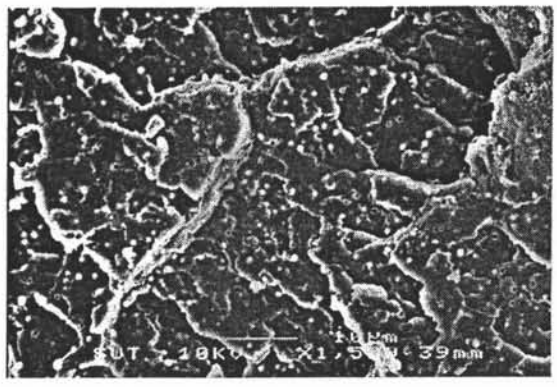

(D) LDPE125KD/95

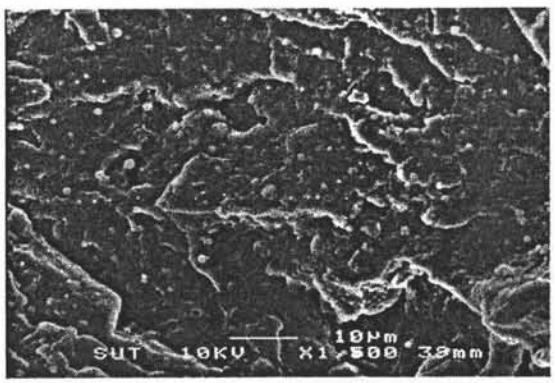

(E) LDPE125KD/95:1

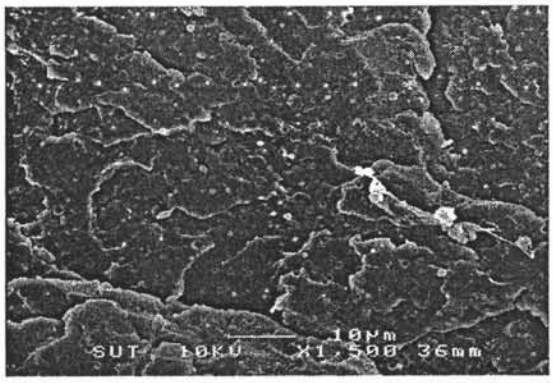

(F) LDPE125KD/95:3

Figure 4.5 Scanning electron micrographs showing the fractured surfaces difference between the uncompatibilized and the compatibilized LDPE125KD/PLA blends by LLDPE-*g*-MA compatibilizer: (A) LDPE125KD/80; (B) LDPE125KD/80:1; (C) LDPE125KD/80:3 (D) LDPE125KD/95; (E) LDPE125KD/95:1; (F) LDPE125KD/95:3

4.3 Thermal analysis of LDPE/PLA blends

4.3.1 DSC measurement

Thermal analysis of the LDPE/PLA blends is shown in Table 4.1 - 4.3 and Figures 4.8 to 4.13. From the DSC thermograms, it can be seen that the melting temperature (T_m) of the blends remains those of the pure component of LDPE240KD, LDPE125KD and PLA. The crystallinity temperature (T_C) and their enthalpy also were investigated in a cooling program after the heating program.

A small effect of the PLA content on T_m of LDPE240KD/PLA and LDPE125KD/PLA was observed. The T_m of the blends designates closely to that of the virgin LDPE, an indication the matrix phase in the blends as present in Figure 4.8(A) and 4.11(A).

Both of the uncompatibilized and compatibilized blends of LDPE240KD/PLA and LDPE125KD/PLA did not show any apparent shift in T_m values that summarize in Table 4.1 and supporting by DSC thermogram in Figure 4.9A, 4.10A, 4.12A and 4.13A. In this study, the two polymers are far from being miscible, the LLDPE-*g*-MA compatibilizer still was not able to bring the two polymer phases to a level of miscibility indicated by the T_m from DSC thermograms. It may be concluded that the LLDPE-*g*-MA is an interfacial agent in this study. Moreover, a slight improvement of compatibility in the SEM study could be observed (Figures 4.4 - 4.5).

The T_C of LDPE125KD/PLA blends increased about 2 °C at 5%PLA addition and maintained at around 94 °C, while a smaller increasing of T_c was found in LDPE240KD virgin as shown in Table 4.2 and Figure 4.8B. The PLA dispersed phase might be affects the creating of spherulite (crystallinity) of LDPE240KD. The compatibilizer effect could not be observed at the small addition amount as present in Figure 4.9B, 4.10. 4.12B and 4.13B but 10 pphr of LLDPE-*g*-MA in LDPE240KD/80:10 exhibit supports of orientation of the polymer chains as a nucleating agent of spherulite.

Enthalpy of melting and crystallization showed a decreasing trend in blends when the amount of PLA was increased but the compatibilizer did not give significant change. The uncompatibilized LDPE240KD/PLA blends also showed the same trend with LDPE125KD/PLA blends with more reducing enthalpy in crystallization as comparison in Figure 4.6 – 4.7. An interesting phenomenon of the compatibilizer effect is to give more enthalpy for decreasing the melting temperature by fewer

energy consume for melting by decreasing 6-7 J/g because of the trends showing the reduced percentages in crystallinity of the compatibilized LDPE 240KD/PLA(Figure 4.6A). Therefore, the enthalpy component from the DSC thermograms can indicate the effect of LLDPE-*g*-MA in the blends.

Table 4.1 T_m of LDPE240KD/PLA and LDPE125KD/PLA blends with various compatibilizer concentrations

LDPE240KD/PLA	**T_m (C^o)**	**LDPE125KD/PLA**	**T_m (C^o)**
PLA(Virgin)	149.89	PLA(Virgin)	149.89
LDPE240KD(Virgin)	109.0	LDPE125K(Virgin)	109.7
LDPE240KD/95	109.0	LDPE125KD/95	110.5
LDPE240KD/95:1	109.0	LDPE125KD/95:1	110.0
LDPE240KD/95:3	109.5	LDPE125KD/95:3	110.5
LDPE240KD/90	108.5	LDPE125KD/90	109.5
LDPE240KD/80	109.0	LDPE125KD/80	109.5
LDPE240KD/80:1	109.0	LDPE125KD/80:1	109.0
LDPE240KD/80:3	109.0	LDPE125KD/80:3	110.5
LDPE240KD/80:10	108.5	-	-

Table 4.2 T_C of LDPE240KD/PLA and LDPE125KD/PLA blends with various compatibilizer concentrations

LDPE240KD/PLA	**T_C (^oC)**	**LDPE125KD/PLA**	**T_C (^oC)**
LDPE240KD(Virgin)	93.5	LDPE125K(Virgin)	92.0
LDPE240KD/95	94.0	LDPE125KD/95	94.0
LDPE240KD/95:1	94.5	LDPE125KD/95:1	94.5
LDPE240KD/95:3	94.5	LDPE125KD/95:3	95.0
LDPE240KD/90	94.0	LDPE125KD/90	94.0
LDPE240KD/80	94.0	LDPE125KD/80	94.0
LDPE240KD/80:1	94.5	LDPE125KD/80:1	95.5
LDPE240KD/80:3	94.5	LDPE125KD/80:3	95.5
LDPE240KD/80:10	96.0	-	-

(A) LDPE240KD, PLA and their blends

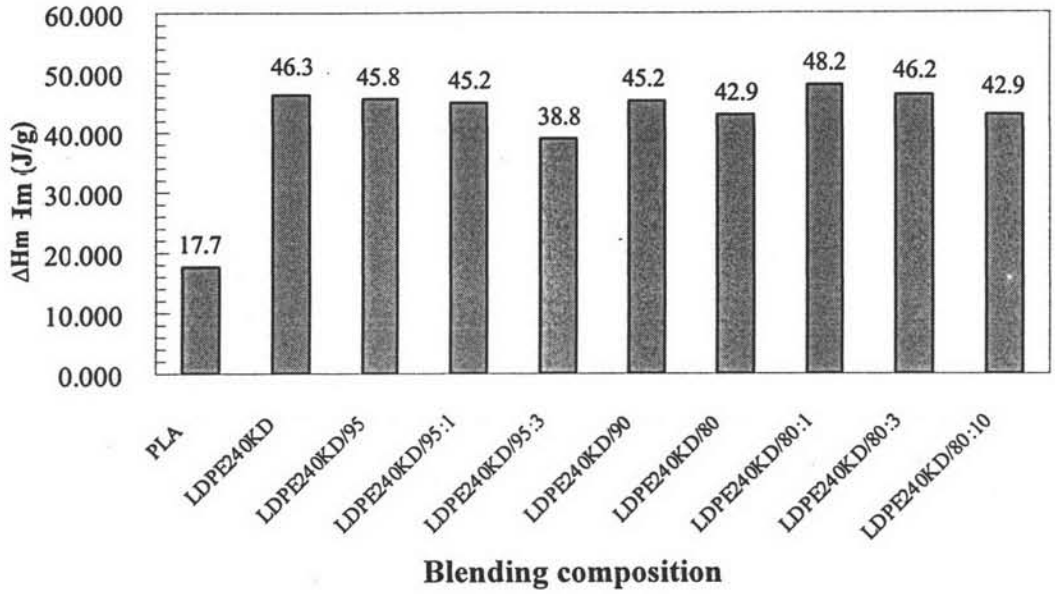

(B) LDPE125KD, PLA and their blends

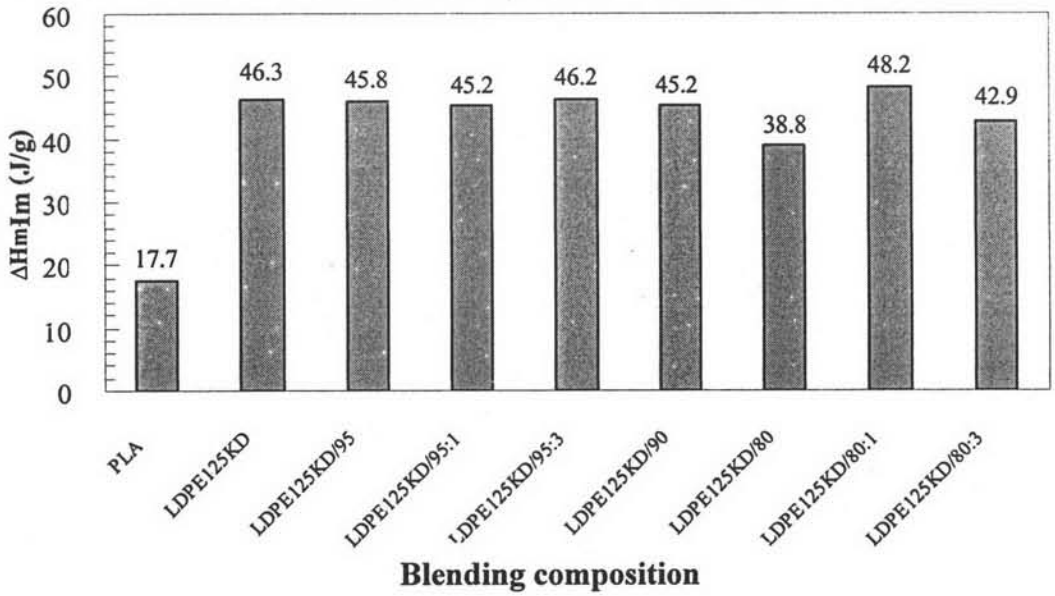

Figure 4.6 Enthalpy of T_m of PLA, LDPE125KD, LDPE240KD and their blends:
(A) LDPE240KD, PLA and their blends;
(B) LDPE125KD, PLA and their blends

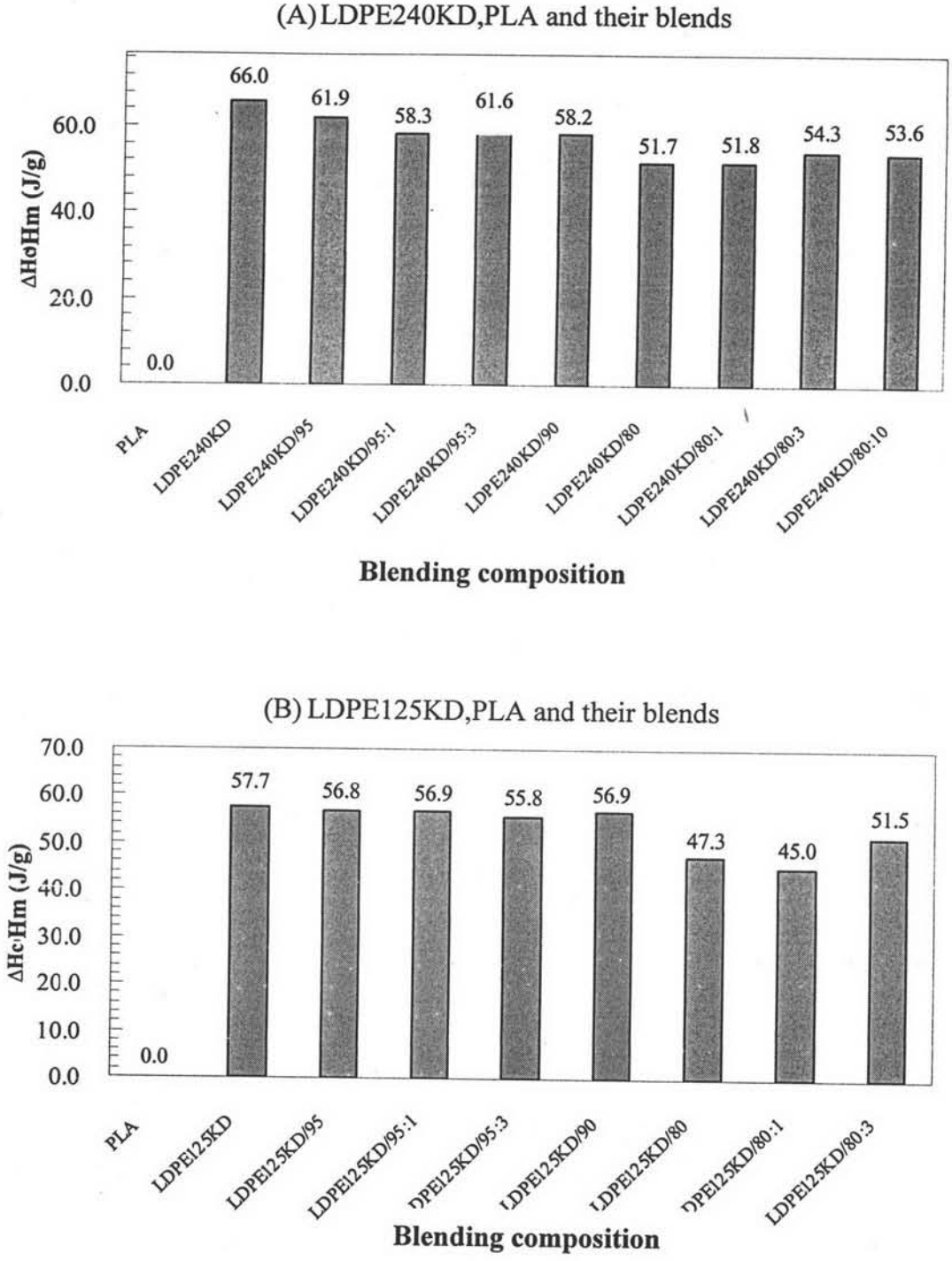

Figure 4.7 Enthalpy T_c of PLA, LDPE125KD, LDPE240KD and their blends

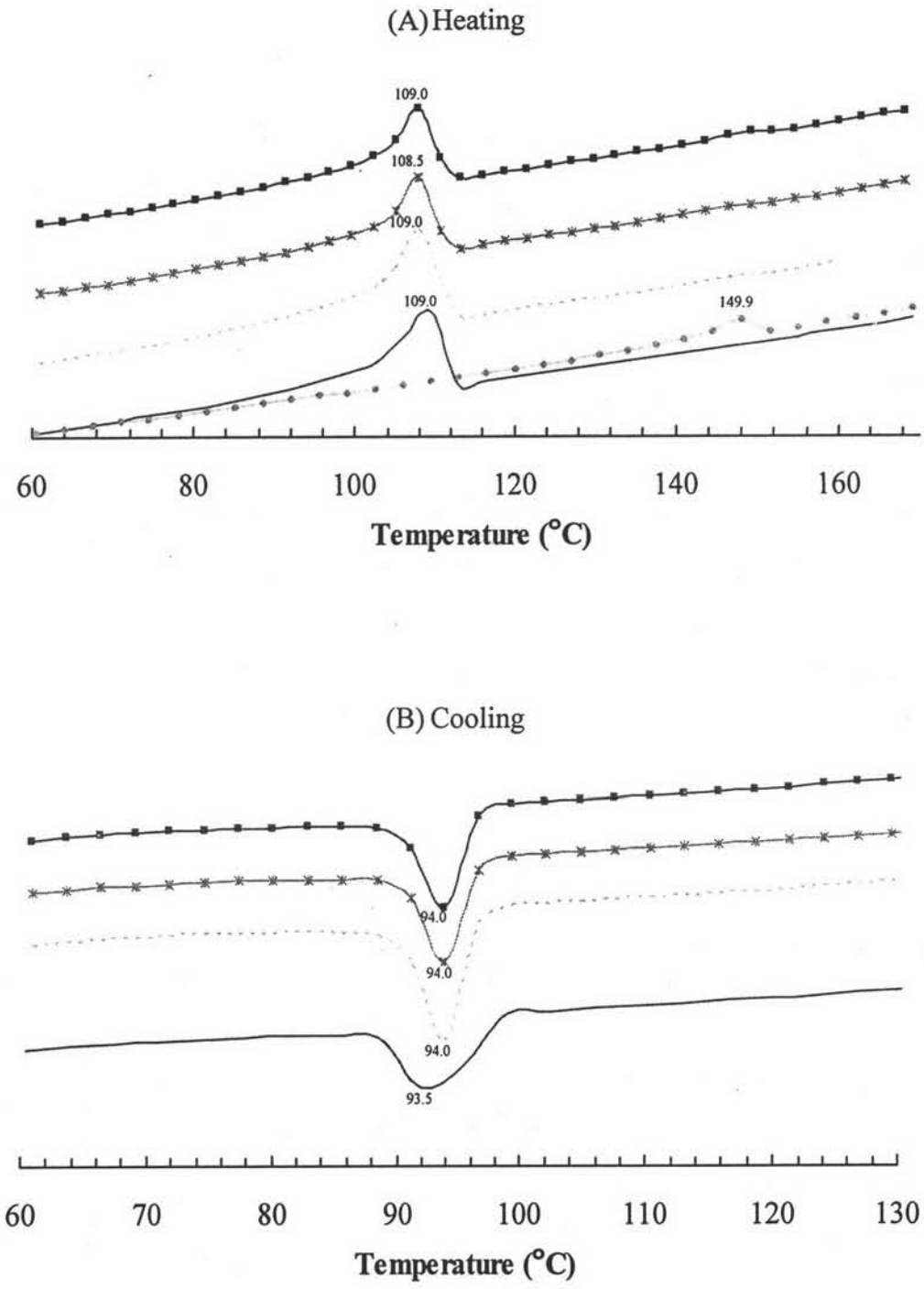

Figure 4.8 DSC thermograms of PLA, LDPE240KD and uncompatibilized LDPE240KD/PLA blends:

PLA — LDPE240KD ····· LDPE240KD/95
LDPE240KD/90 — LDPE240KD/80

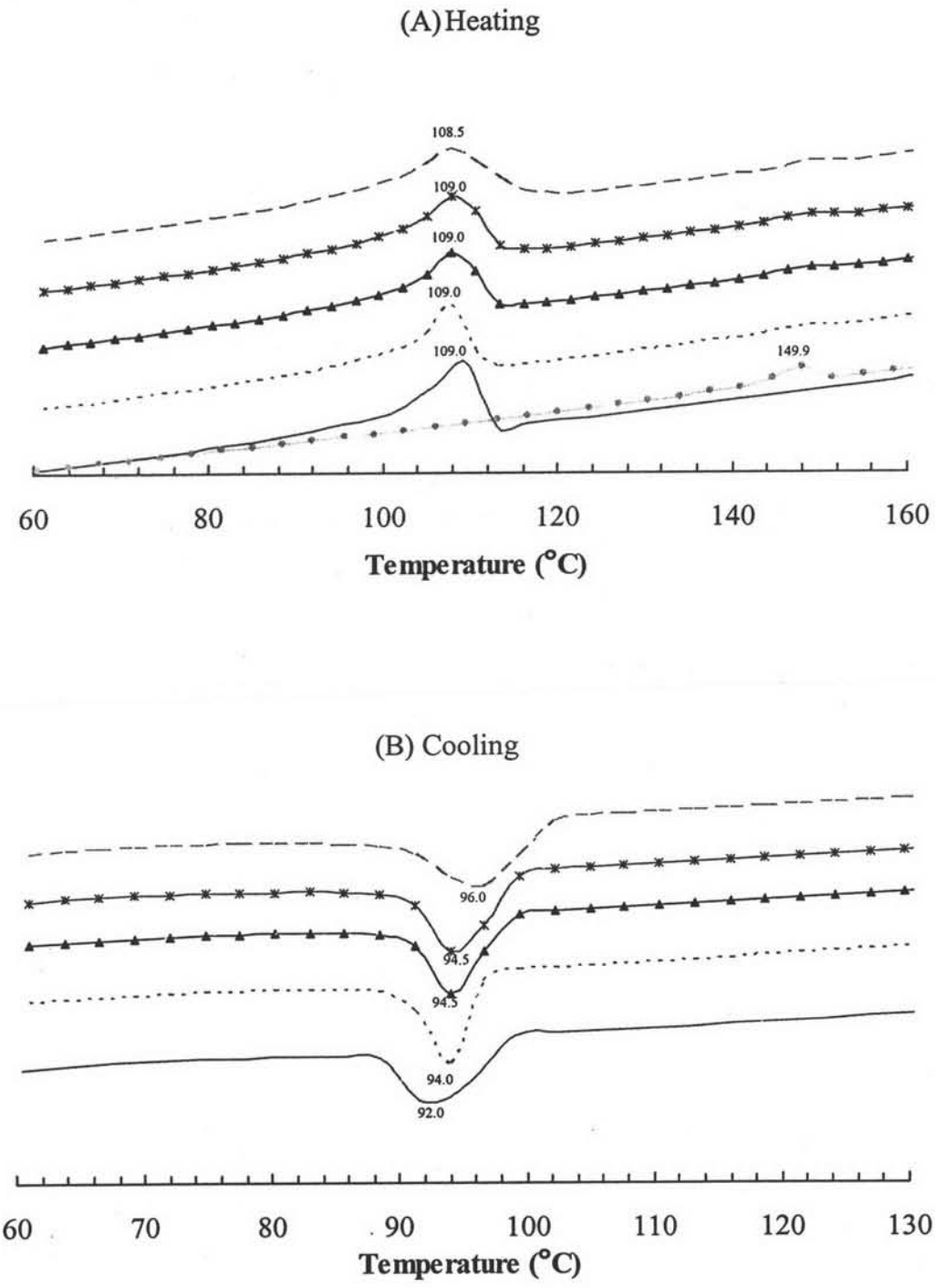

Figure 4.9 DSC thermograms of PLA, LDPE240KD, LDPE240KD/80 blends uncompatibilized and compatibilized with LLDPE-g-MA:

PLA — LDPE240KD ····· LDPE240KD/80
LDPE240KD/80:1 — LDPE240KD/80:3 - - - - LDPE240KD/80:10

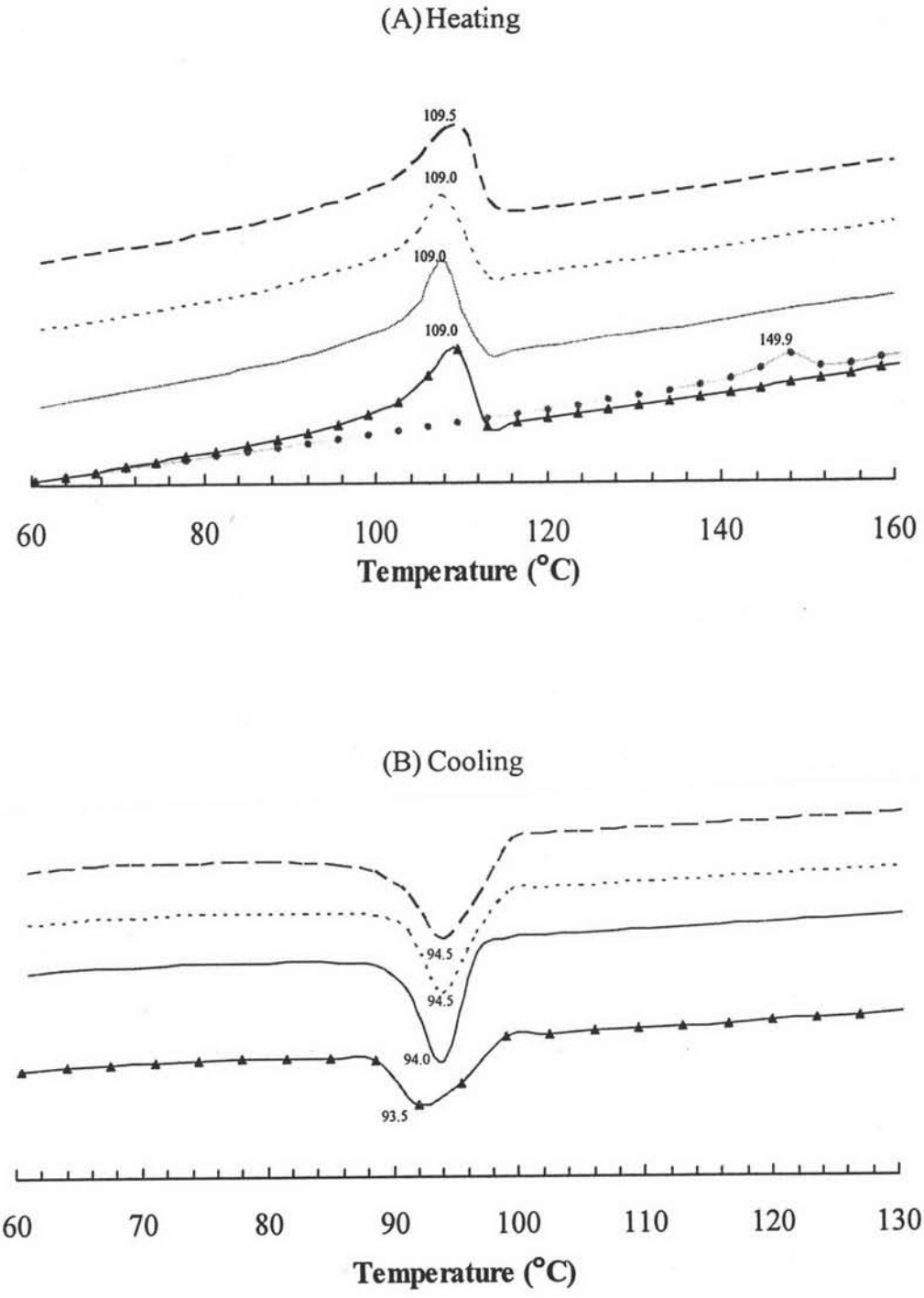

Figure 4.10 DSC thermograms of PLA, LDPE240KD, LDPE240KD/95 blends uncompatibilized and compatibilized with LLDPE-g-MA:

PLA — LDPE240KD — LDPE240KD/95
LDPE240KD/95:1 - - - LDPE240KD/95:3

(A) Heating

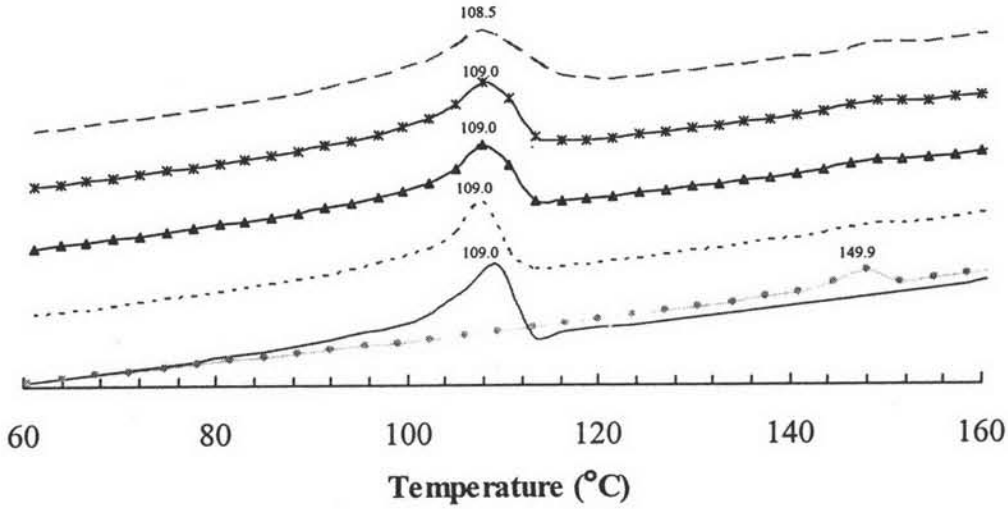

(B) Cooling

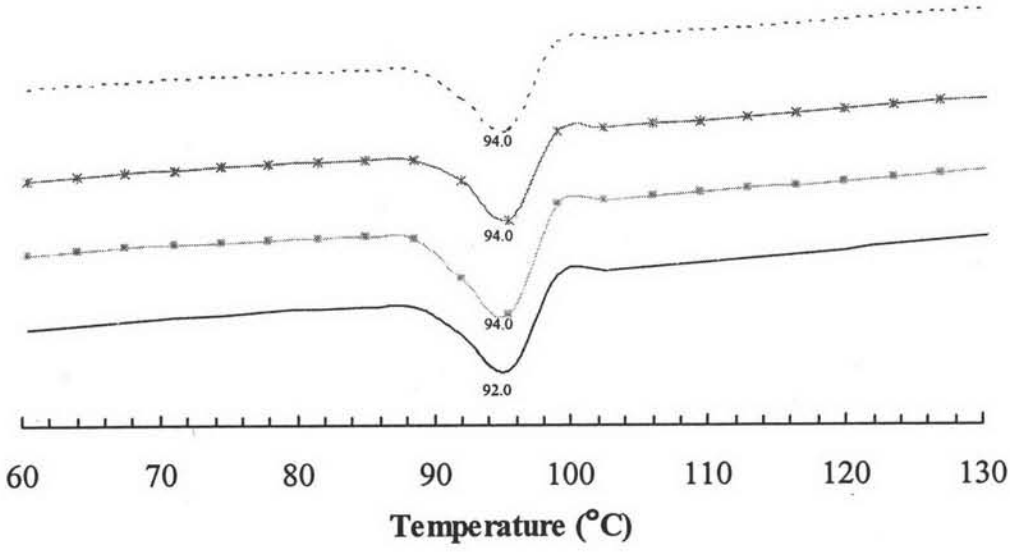

Figure 4.11 DSC thermograms of PLA, LDPE125KD and uncompatibilized LDPE125KD/PLA blends:

PLA — LDPE125KD — LDPE125KD/95
LDPE125KD/90 ····· LDPE125KD/80

(A) Heating

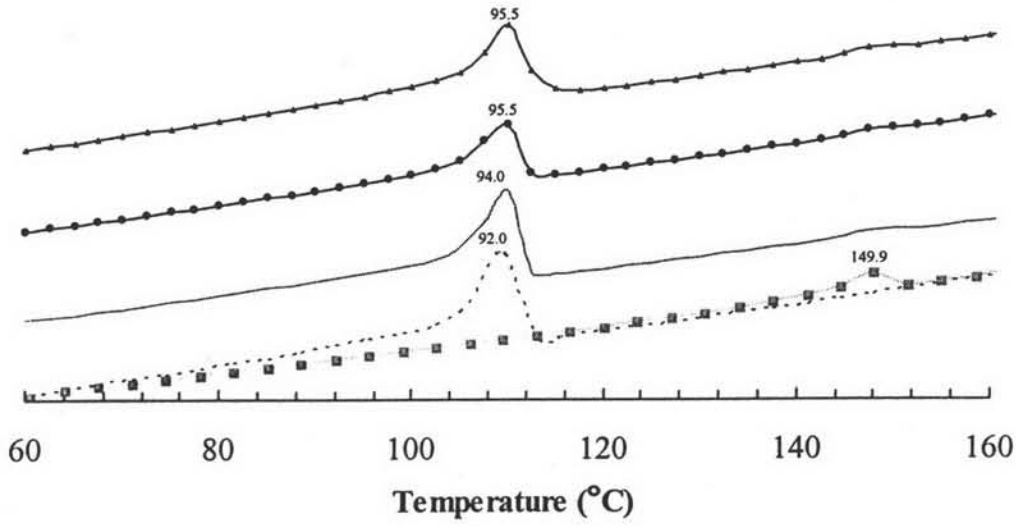

(B) Cooling

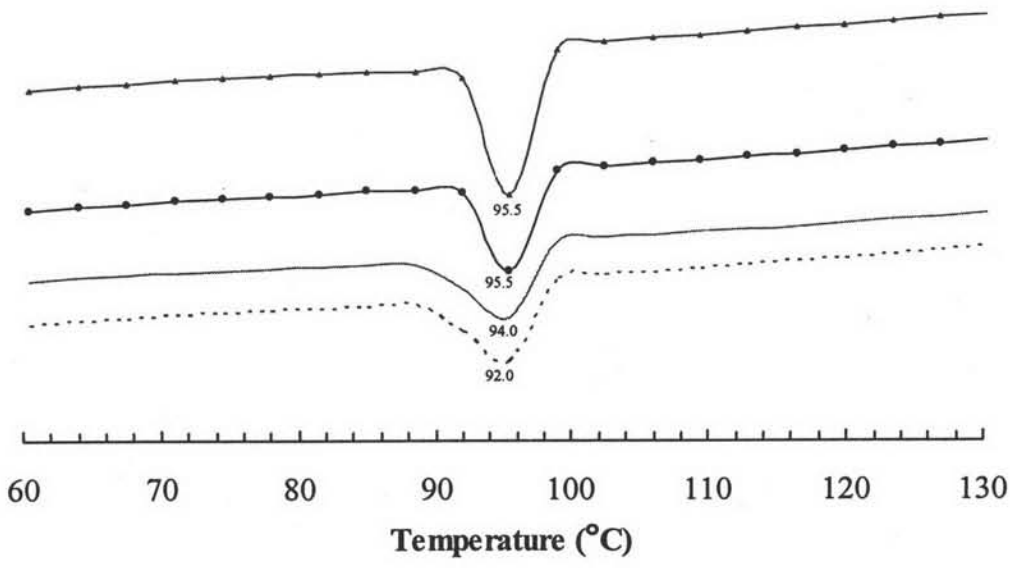

Figure 4.12 DSC thermograms of PLA, LDPE125KD, LDPE125KD/80 blends uncompatibilized and compatibilized with LLDPE-g-MA:

PLA ····· LDPE125KD ——— LDPE125KD/80
—•— LDPE125KD/80:1 —•— LDPE125KD/80:3

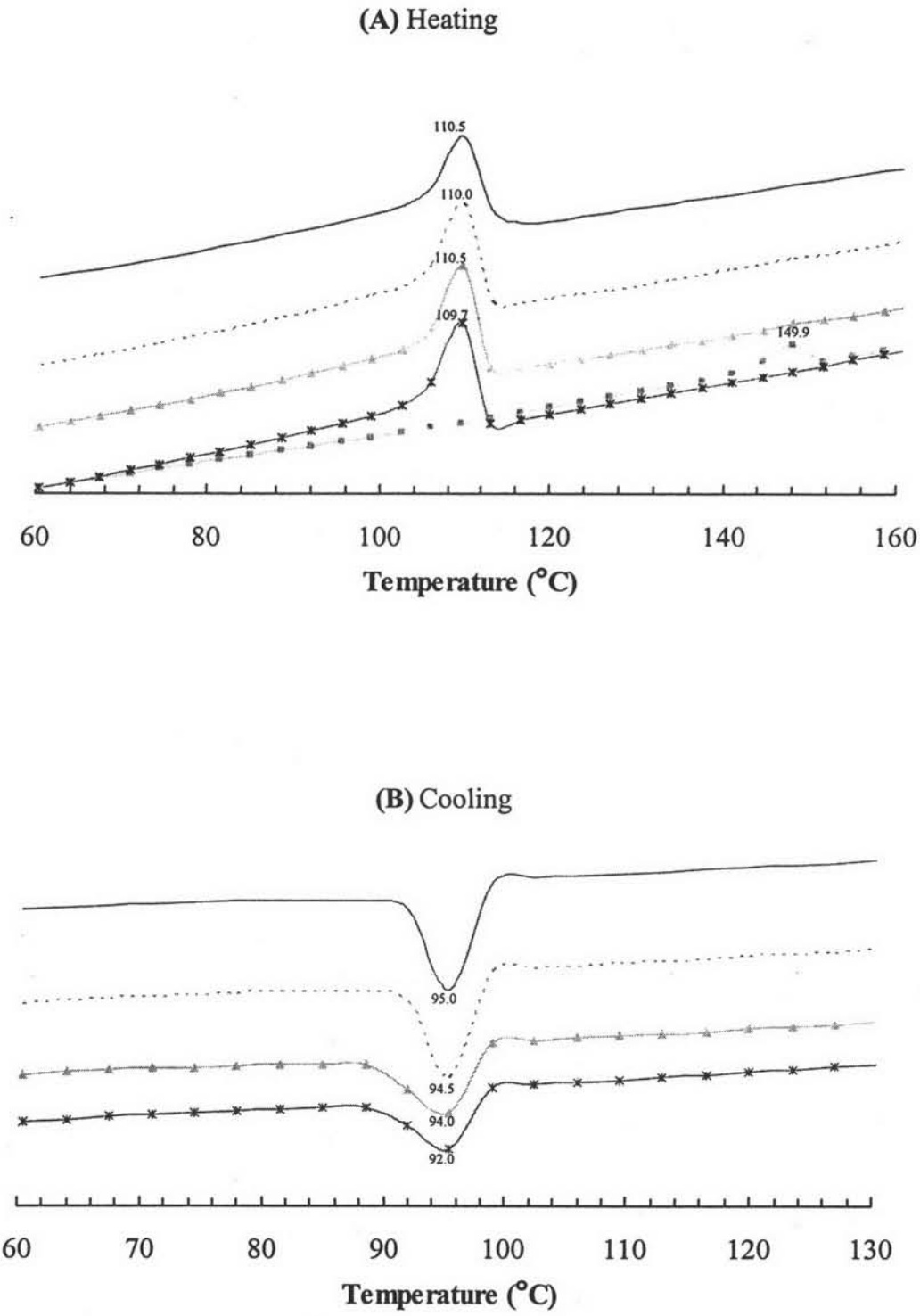

Figure 4.13 DSC thermograms of PLA, LDPE125KD, LDPE125KD/95 blends uncompatibilized and compatibilized with LLDPE-*g*-MA:

4.3.2 TGA measurement

Table 4.3 and Figure 4.14 to 4.20 show results from TGA thermograms of LDPE240KD/PLA and LDPE125KD/PLA blends. The degradation temperature(T_d) of all blend exhibits some extent of increasing after PLA content from addition of 5-20%PLA and n further change was observed at 1-3 pphr of compatibilizer. However, for LDPE240KD/80:10 has lower thermal stability due to PLA was grafted on LDPE molecular chain and then stability of LDPE chain might be effected. Effect of molecular weight change when comparison between LDPE125KD/80 and LDPE240KD/80 in Figure 2.10 cannot detect and also in Figure 2.21 of their compatibilized blends don't show significant difference.

Table 4.3 T_d of LDPE240KD/PLA and LDPE125KD/PLA blends with various compatibilizer concentrations

LDPE240KD/PLA	**T_d (C^o)**	**LDPE125KD/PLA**	**Td (C^o)**
PLA(Virgin)	370	PLA(Virgin)	370
LDPE240KD(Virgin)	480	LDPE125K(Virgin)	480
LDPE240KD/95	485	LDPE125KD/95	485
LDPE240KD/95:1	485	LDPE125KD/95:1	485
LDPE240KD/95:3	485	LDPE125KD/95:3	485
LDPE240KD/90	485	LDPE125KD/90	485
LDPE240KD/80	485	LDPE125KD/80	485
LDPE240KD/80:1	485	LDPE125KD/80:1	485
LDPE240KD/80:3	485	LDPE125KD/80:3	485
LDPE240KD/80:10	480	-	-

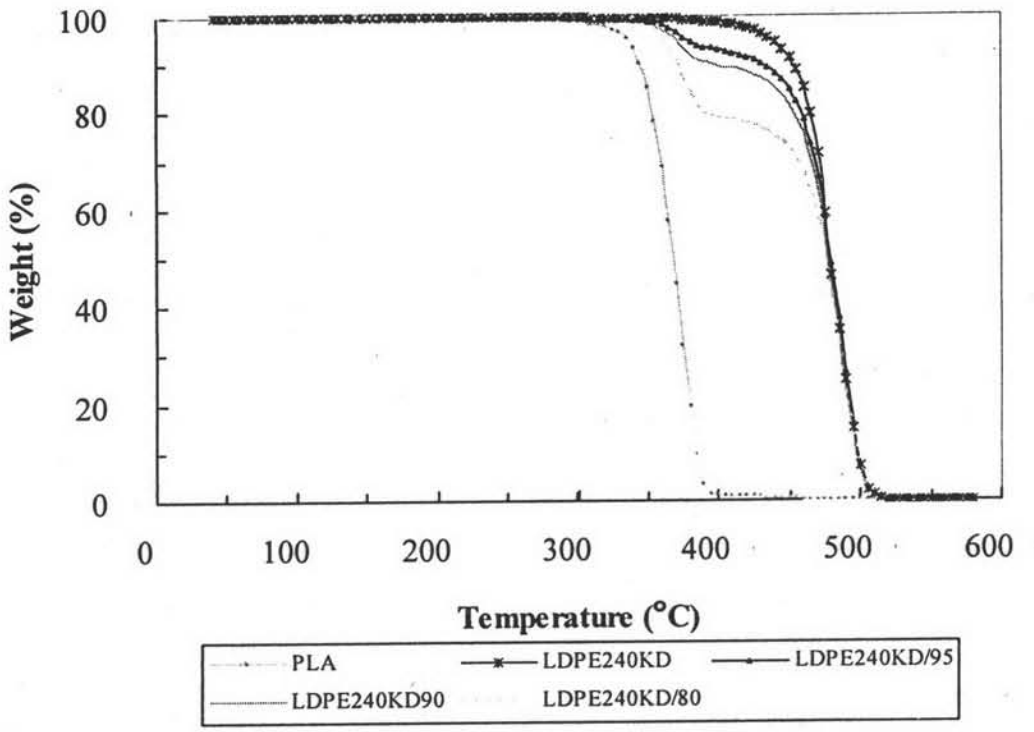

Figure 4.14 DMTA of PLA, LDPE240KD and the uncompatibilized LDPE240KD/PL blends.

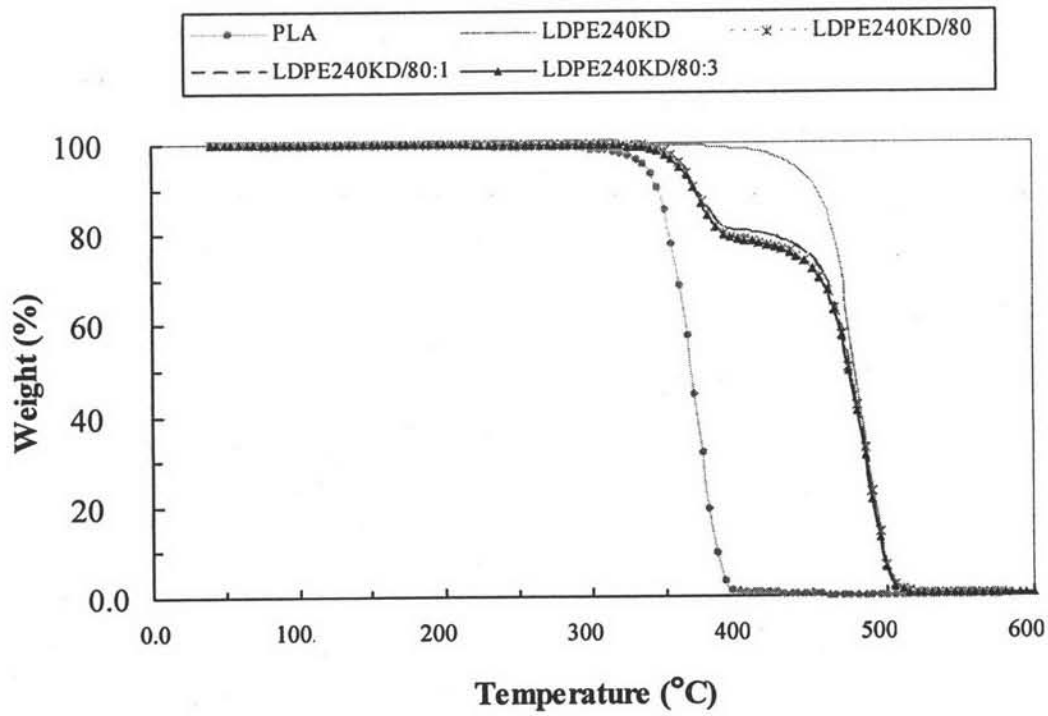

Figure 4.15 DMTA of PLA, LDPE240KD and the compatibilized/uncompatibilized LDPE240KD/80 blends.

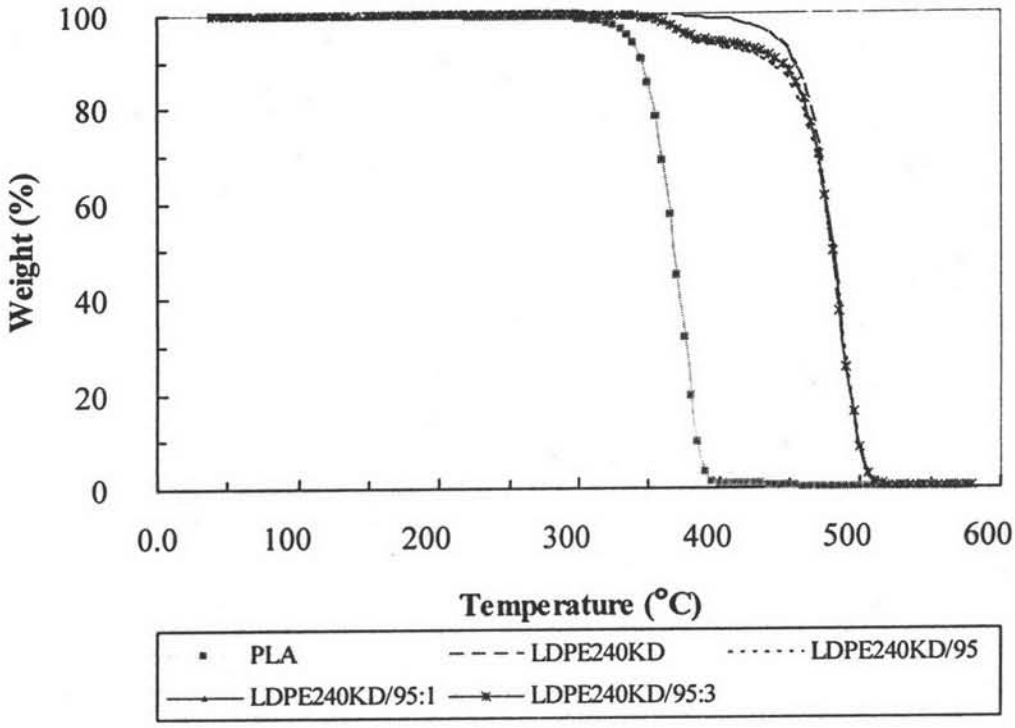

Figure 4.16 DMTA of PLA, LDPE240KD and the compatibilized/uncompatibilized LDPE240KD/95 blends.

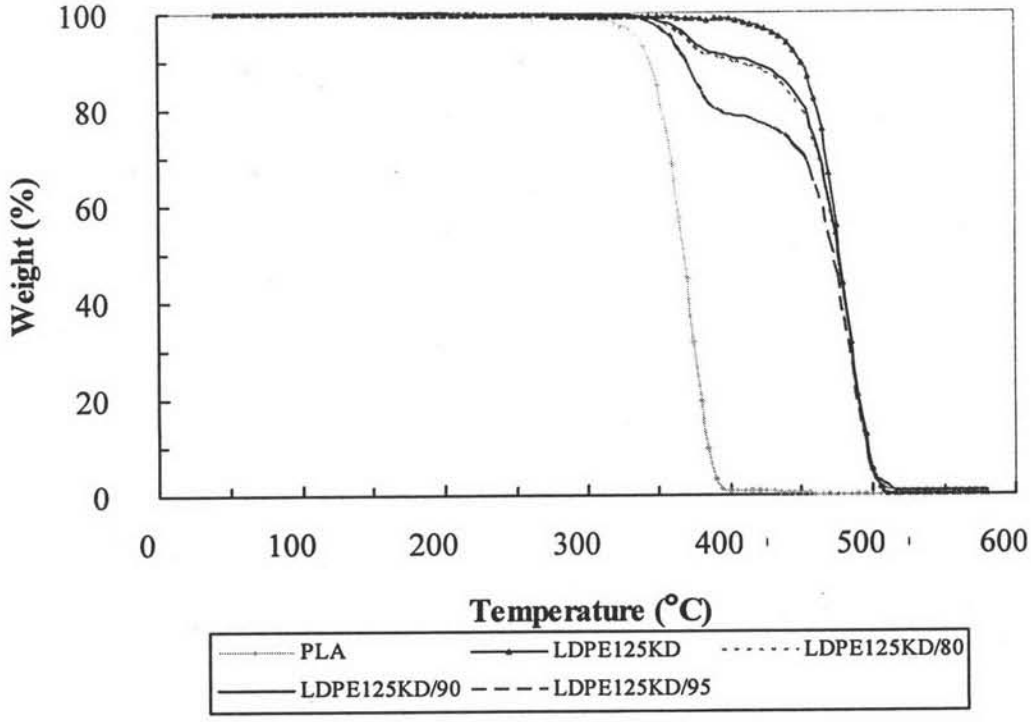

Figure 4.17 DMTA of PLA, LDPE125KD and the uncompatibilized LDPE125KD/PLA blends.

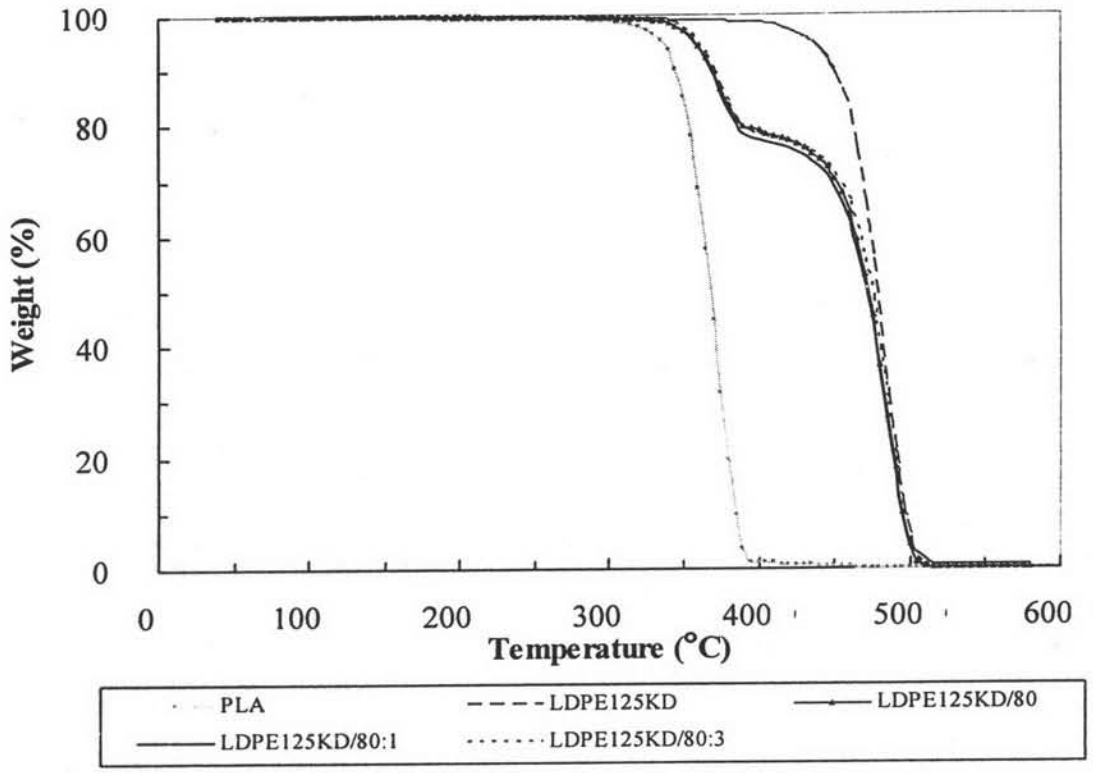

Figure 4.18 DMTA of PLA, LDPE125KD and the compatibilized/uncompatibilized LDPE125KD/80 blends.

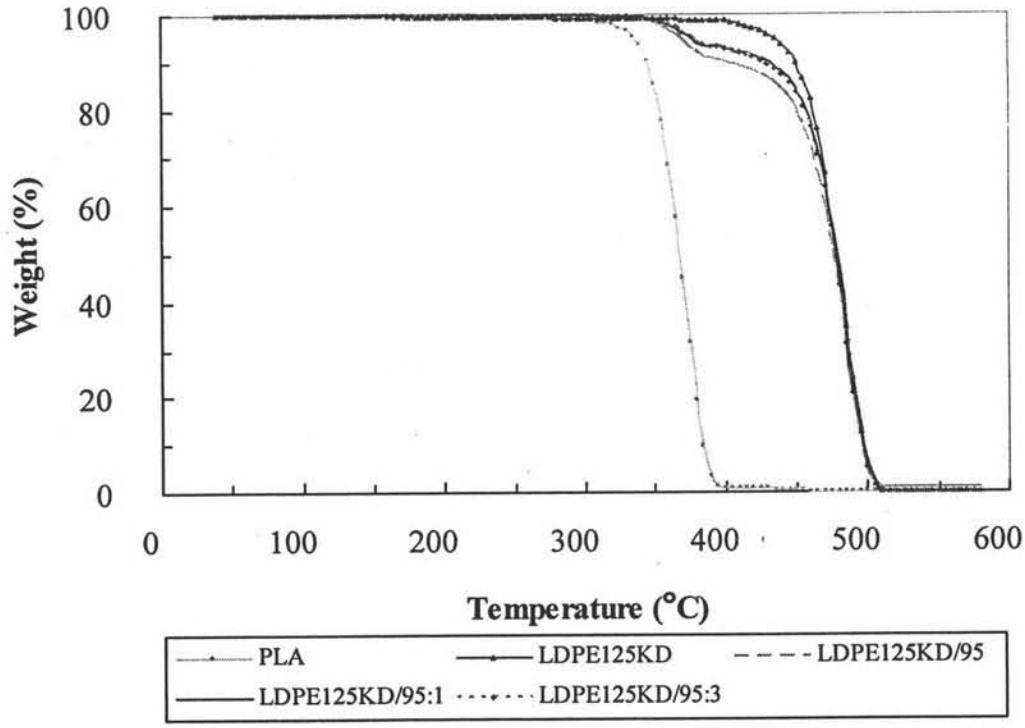

Figure 4.19 DMTA of PLA, LDPE125KD and the compatibilized/uncompatibilized LDPE125KD/80 blend

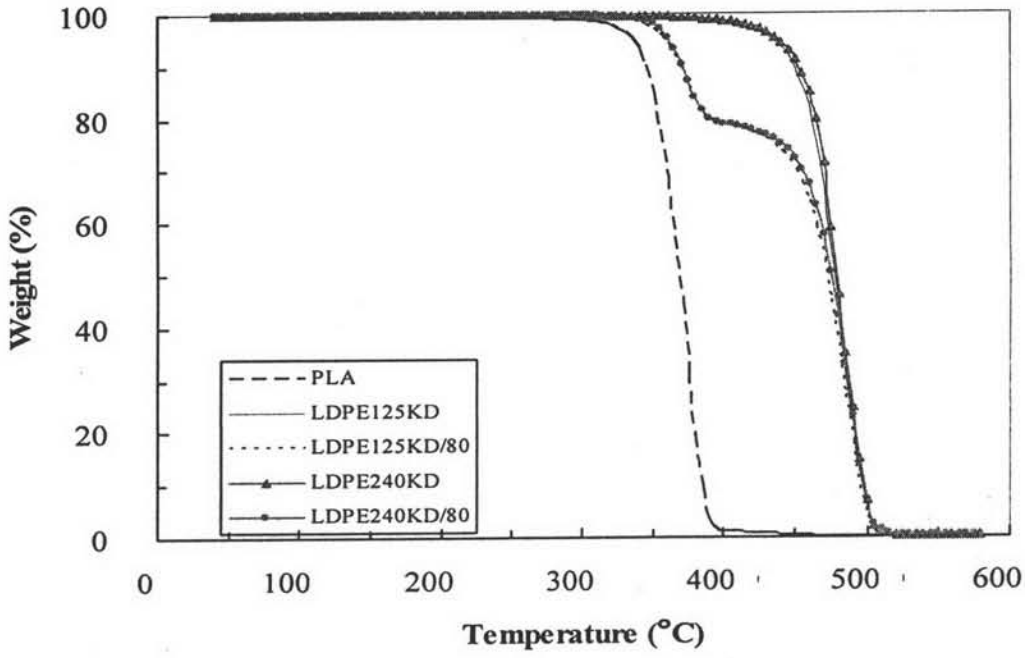

Figure 4.20 Comparison of DMTA for PLA, LDPEs and their uncompatibilized blends at PLA 20% content

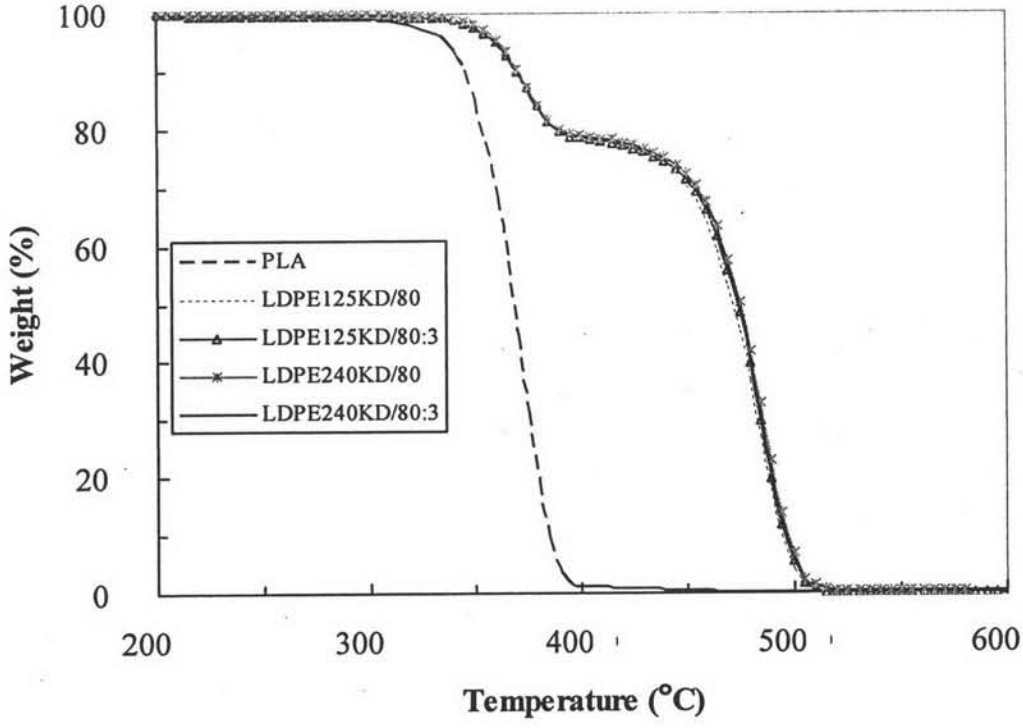

Figure 4.21 Comparison of DMTA between PLA and their compatibilized/uncompatibilized blends of LDPE/PLA blends at PLA 20% contents with 3 pphr compatibilizer

4.4 Mechanical blends properties of LDPE/PLA

Generally, it has been known for a long time that immiscible polymer blends have inferior mechanical properties due to the existence of weak interfacial adhesion and poor dispersion of the component. In this study, the mechanical properties for the molecular weight difference of LDPE on the LDPE240KD/PLA and LDPE125KD/PLA blends by LLDPE-*g*-MA as compatibilizer on the impact strength and tensile strength are investigated.

4.4.1 Impact strength of TPE/PLA blends

Izod impact strength data of LDPE240KD/PLA and LDPE125KD/PLA blends of the uncompatibilized and compatibilized with LLDPE-*g*-MA are shown in Table 4.4. It can be seen that the Izod impact strength of the uncompatibilized LDPE240KD/PLA blends is slightly reduced in comparison with virgin LDPE and become poor by 70% reduction at 20%PLA addition because PLA has lower impact strength. Beside, this indicates the poor interfacial adhesion between the two phases. The LDPE125KD/95 and LDPE125KD/90 blends have high impact strength compared with the virgin LDPE This could be caused by the microphase of PLA performing as reinforce particle according to it has high stiffness as can be seen in SEM (Figure 4.3 (F) and (G)). The LDPE125KD/80 blend has agglomerates of PLA molecular chains so the morphology affects impact strength reduction more than relatively 30%. Increases in the LLDPE-*g*-MA content in each blend ratio improves impact strength of the LDPE240KD/PLA blends. This is might be due to the fact that the phase morphology was improved and the dispersed phase became much finer which molecular size of LDPE240KD is lager and its molecular chain energy could resist impact force than LDPE15KD which PLA molecular size comparison with LDPE125KD is smaller that internal bond energy is not much resist the impact force as much as LDPE240KD matrix.

Table 4.4 Izod impact strength of LDPE240KD/PLA and LDPE125KD/PLA blends with various compatibilizer concentrations

LDPE240KD/PLA	Impact strength (kJ/ m^2)	**LDPE125KD/PLA**	Impact strength (kJ/ m^2)
PLA(Virgin)	3.57±2.31	PLA(Virgin)	3.57±2.31
LDPE240KD(Virgin)	42.90±3.11	LDPE125K(Virgin)	30.17±2.62
LDPE240KD/95	41.34±7.06	LDPE125KD/95	39.36±3.72
LDPE240KD/95:1	41.11±5.45	LDPE125KD/95:1	37.31±4.01
LDPE240KD/95:3	42.93±3.42	LDPE125KD/95:3	34.78±3.60
LDPE240KD/90	40.00±2.38	LDPE125KD/90	37.09±1.81
LDPE240KD/80	9.94±1.08	LDPE125KD/80	19.50±2.37
LDPE240KD/80:1	12.51±0.93	LDPE125KD/80:1	12.51±2.08
LDPE240KD/80:3	11.9±0.55	LDPE125KD/80:3	9.22±0.85
LDPE240KD/80:10	10.45±0.93	-	-

4.4.2 Tensile strength of TPI/PLA blends

It is worthwhile to mention that the uncompatibilized single polymer (PLA alone) has higher tensile strength than LDPE. The single polymer provides its unique property for a particular application. Each virgin polymers indicate tensile properties in Figure 4.22 in which PLA is brittle but has very high stiffness and LDPE125KD has more elongation and more ductile than LDPE240KD. Tensile strength results are shown in Table 4.5 and Figures 4.20 - 4.22. The tensile strength show slightly increases at 20%PLA blending in LDPE125KD/PLA. Likewise, addition of LLDPE-g-MA shows a similar trend to which promote tensile strength (Figure 4.23-4.24) which is increased with the increasing compatibilizer amount (1, 3 and 10 pphr) in LDPE240KD/20.

The yield stress value gives an increasing trend with increasing amount of PLA in both LDPE240KD/PLA and LDPE125KD/PLA blends and is significantly increased at LDPE240KD/20:10. Yong's modulus increase when PLA content increased. Both of them illustrate that LLDPE-g-MA decreases relative Yong's moduli at 20%PLA content as shown in Figure 4.25(B) To observe the effect by %

relative change by compare with those of polymer matrix properties and fond that mostly effect to mechanical properties which relate to the entanglement of molecular chain.

Another tensile property, elongation at break of LDPE240KD/PLA and LDPE125KD/PLA blends yield lower values when increasing concentration of PLA. The elongation at break for these blend ratios illustrates the result of poor dispersibility of PLA domain in both types of LDPE matrix polymers. For the compatibilized LDPE240KD/PLA blends with LLDPE-g-MA, elongation at break increases with the LLDPE-g-MA concentration. Although LDPE125KD/PLA blend at 95%PLA does not change much, the increasing elongation at break is observed at 20%PLA. It is possibly claimed that the LLDPE-g-MA can, nevertheless, enhance somewhat interfacial adhesion of the phase boundaries between the two polymers. However, LDPE240KD/PLA blends indicate more elongation of PLA than LDPE125KD/PLA blends.

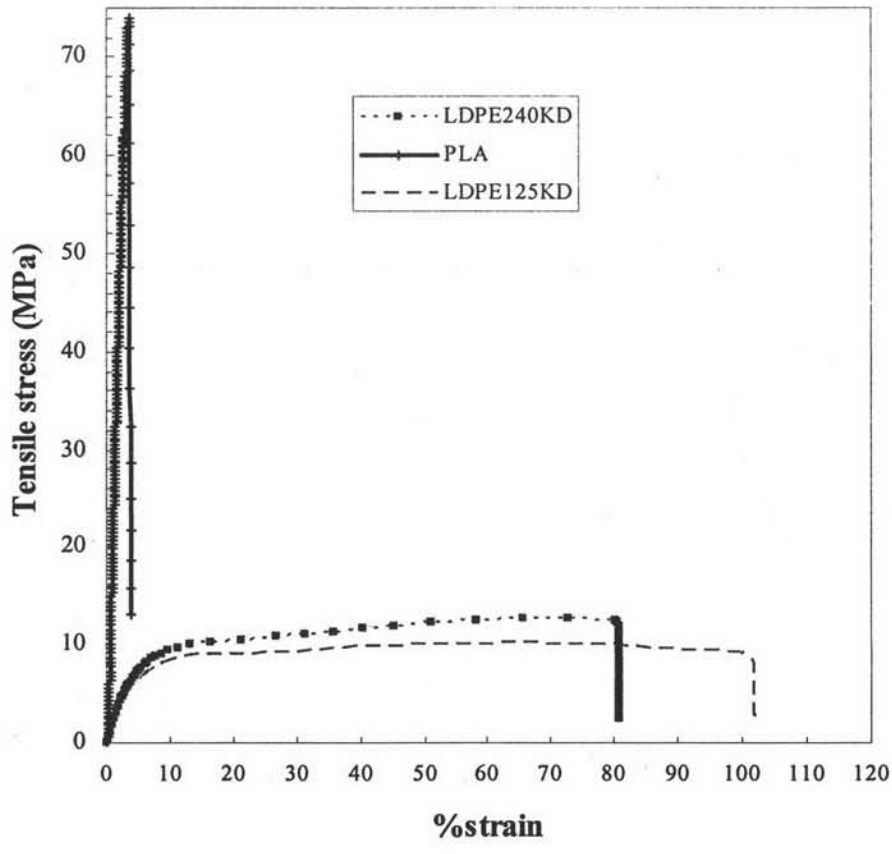

Figure 4.22 Tensile strength of PLA, LDPE125KD and LDPE240KD

Table 4.5 Mechanical properties of LDPE240KD/PLAblends with various compatibilizer concentrations

Blend composition	Young's modulus (M Pa)	Tensile strength (M Pa)	Yield stress (M Pa)	Elongation (%)
PLA(Virgin)	2905.23±11.3	73.77±0.14	44.95±0.13	3.63±4.60
LDPE240KD	256.23±16.41	13.50±0.23	7.53±0.19	94.10±1.73
LDPE240KD/95	294.73±10.20	13.19±0.40	8.26±0.15	78.17±1.99
LDPE240KD/95:1	304.97±6.01	13.56±0.15	8.05±0.09	80.36±1.78
LDPE240KD/95:3	310.04±7.38	13.04±0.35	7.96±0.10	81.50±5.20
LDPE240KD/90	363.13±19.22	11.81±0.20	9.60±0.20	47.05±2.90
LDPE240KD/80	529.60±18.33	12.40±0.16	12.48±0.13	11.83±1.22
LDPE240KD/80:1	524.71±14.20	12.96±0.21	12.75±0.15	16.12±3.08
LDPE240KD/80:3	506.62±26.14	13.13±0.27	12.88±0.26	20.65±4.27
LDPE240KD/80:10	496.00±35.69	13.45±0.33	13.22±0.28	34.72±4.78

Table 4.6 Mechanical properties of LDPE125KD/PLA blends with various compatibilizer concentrations

Blend composition	Young's modulus (M Pa)	Tensile strength (M Pa)	Yield stress (M Pa)	Elongation (%)
PLA(Virgin)	2905.23±11.3	73.77±0.14	44.95±0.13	3.63±4.60
LDPE125KD	220.97±16.52	9.08±0.12	6.18±0.13	111.02±4.80
LDPE125KD/95	250.46±11.95	8.98±0.16	6.56±0.13	108.91±6.89
LDPE125KD/95:1	263.18±11.83	9.15±0.14	6.98±0.14	96.02±6.35
LDPE125KD/95:3	282.51±6.13	9.53±0.14	7.15±0.09	94.09±2.47
LDPE125KD/90	292.65±13.92	8.32±0.16	7.31±0.05	77.34±11.62
LDPE125KD/80	483.79±24.91	10.28±0.18	10.25±0.24	34.75±4.25
LDPE240KD/80:1	444.46±20.20	10.30±0.17	10.21±0.21	43.54±4.90
LDPE125KD/80:3	451.51±33.72	10.33±0.19	10.57±0.43	49.48±6.04

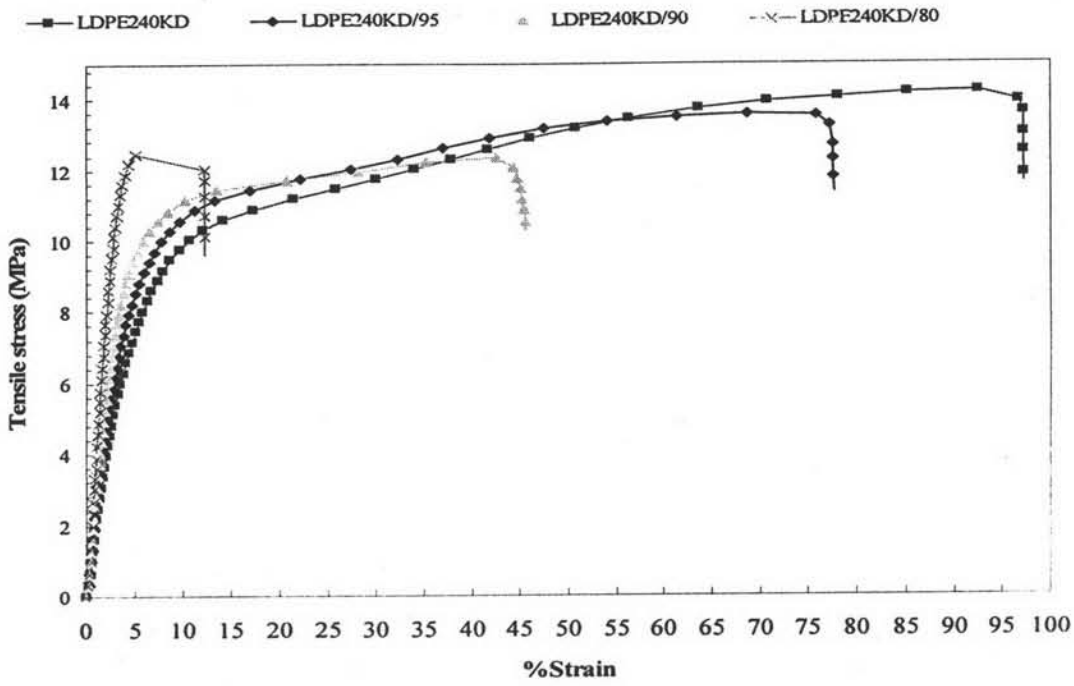

(A) LDPE240KD/PLA

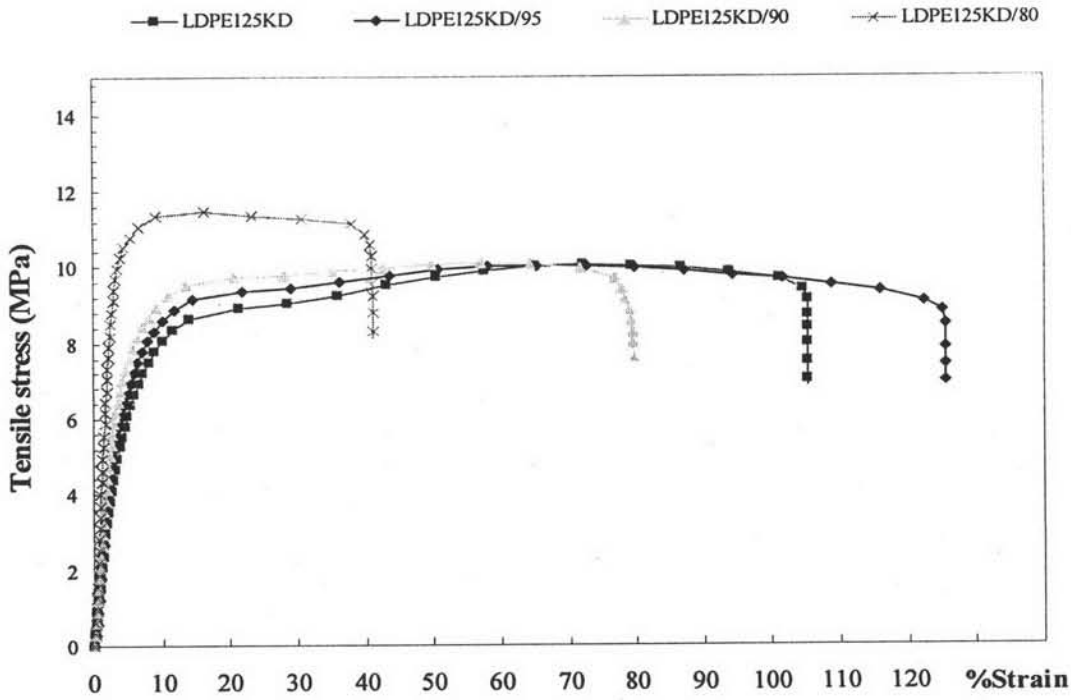

(B) LDPE125KD/PLA

Figure 4.23 Tensile strength of LDPE240KD/PLA and LDPE125KD/PLA blends with various PLA contents

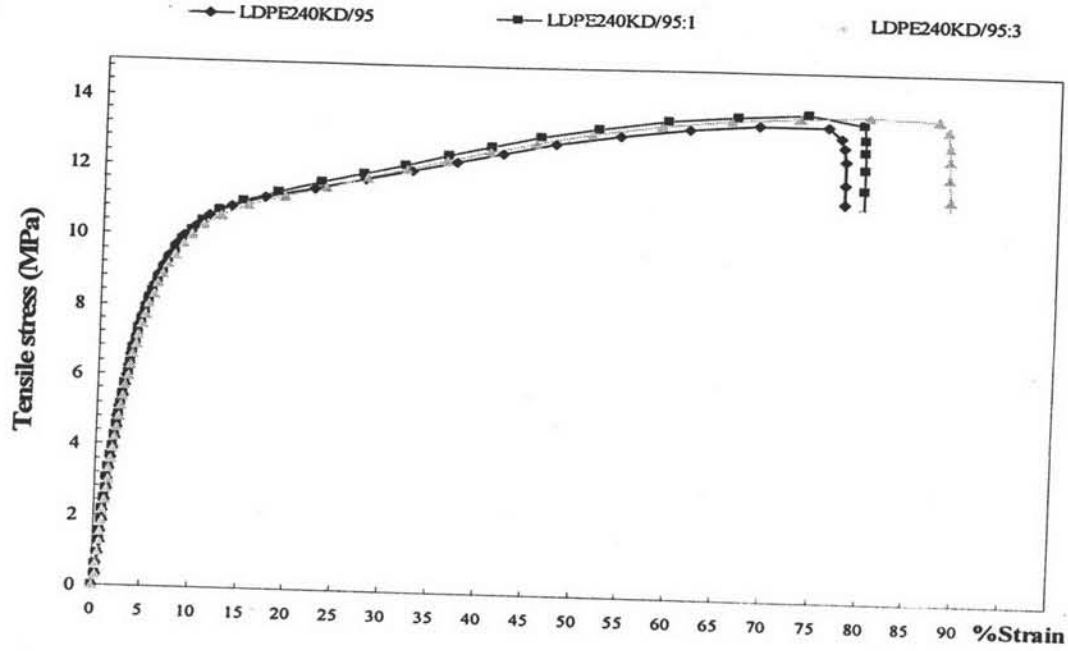

(A) The uncompatibilized and compatibilized LDPE240KD/95 blends

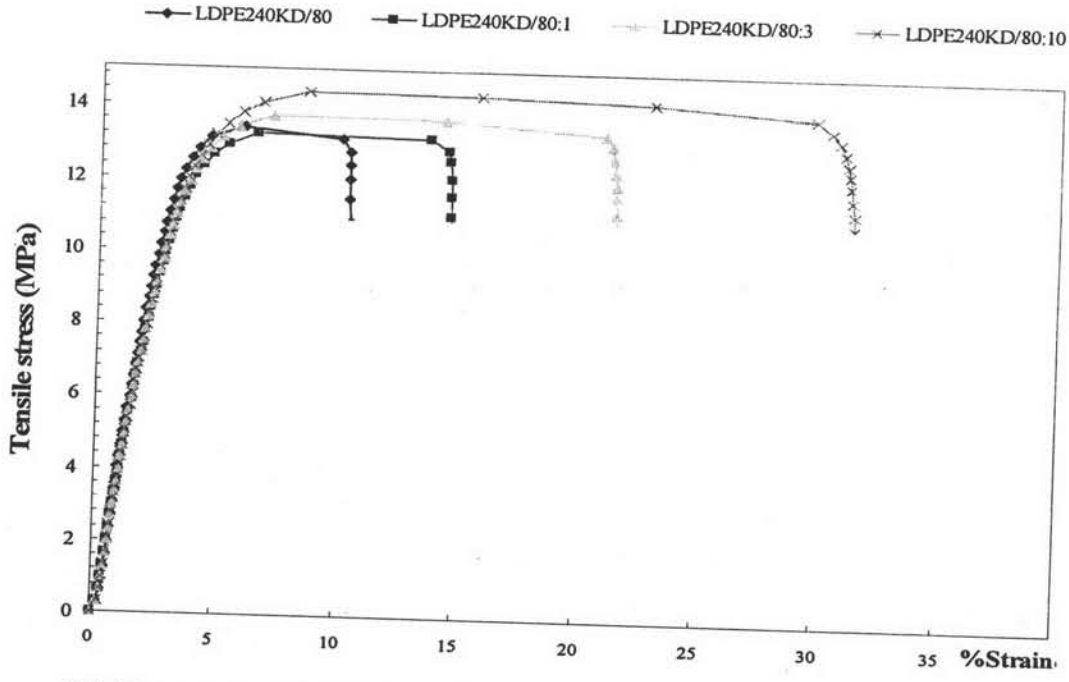

(B) The uncompatibilized and compatibilized LDPE240KD/80 blends

Figure 4.24 Tensile strength of the uncompatibilized and compatibilized LDPE240KD/95 blends with 1 pphr and 3 pphr of LLDPE-*g*-MA

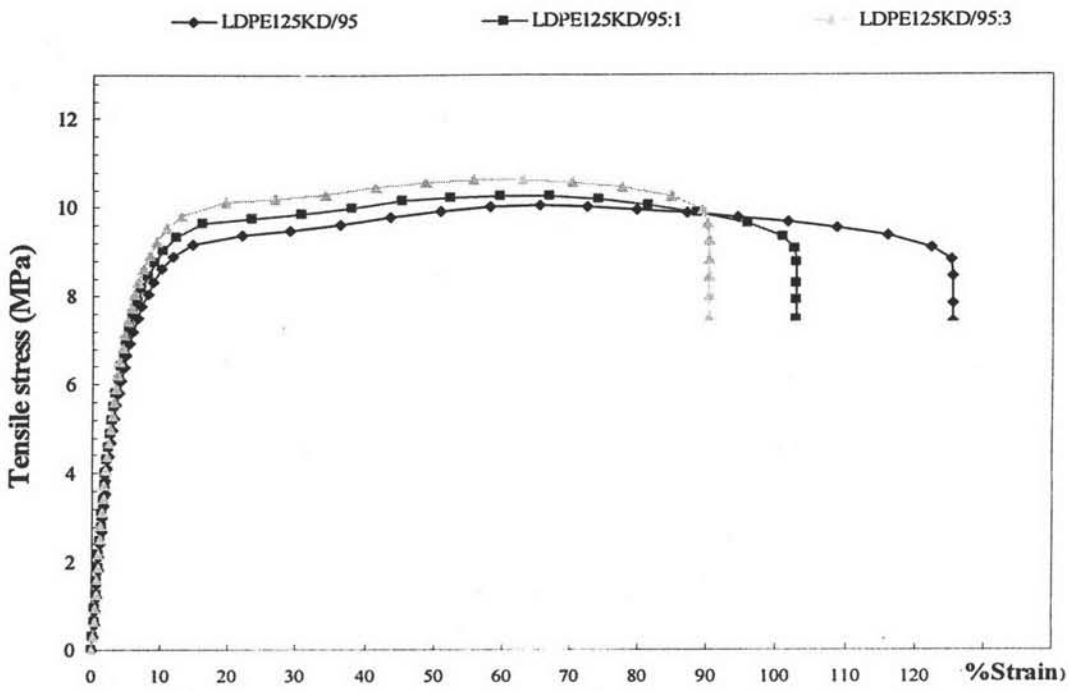

(A) The uncompatibilized and compatibilized LDPE125KD/95 blends

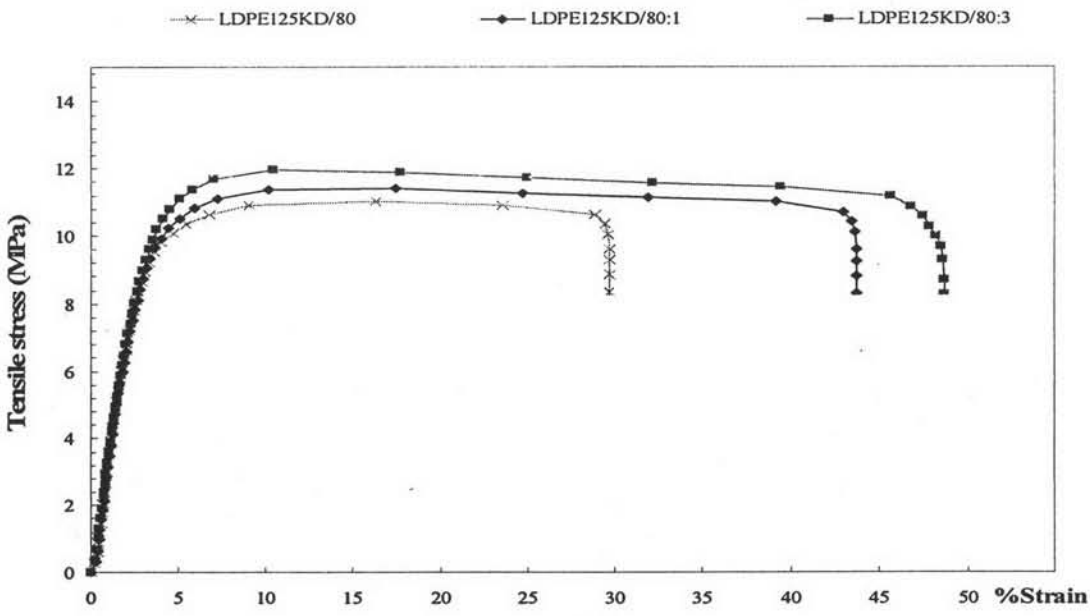

(B) The uncompatibilized and compatibilized LDPE125KD/80 blends

Figure 4.25 Tensile strength of the uncompatibilized and compatibilized LDPE125KD/95 blends with 1 pphr and 3 pphr of LLDPE-*g*-MA

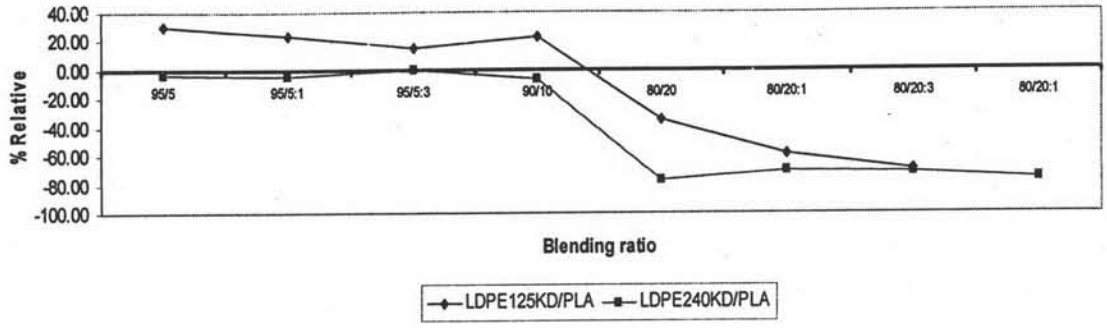

(A) Relative impact strength

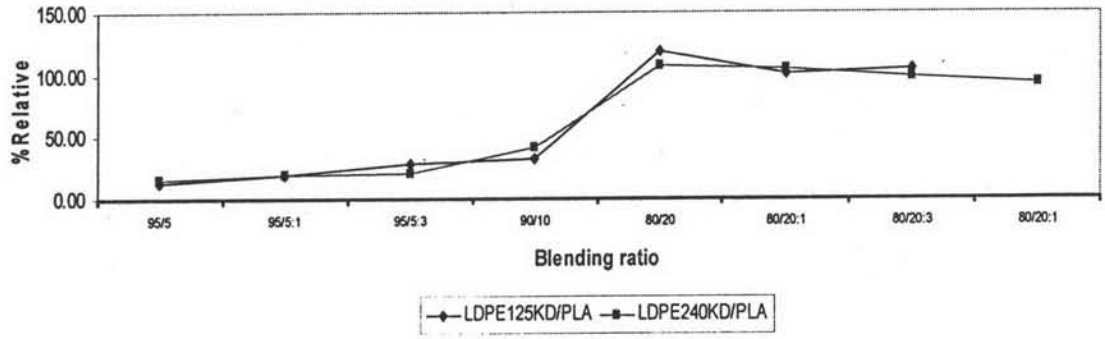

(B) Relative Yung's modulus

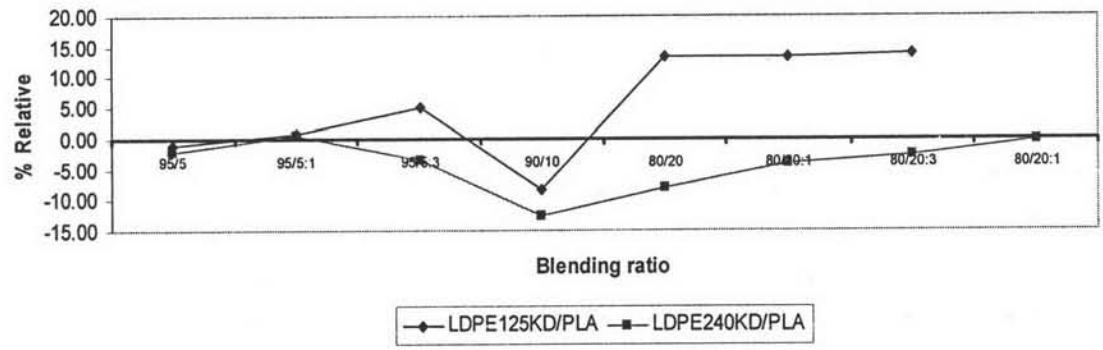

(C) Relative maximum tensile

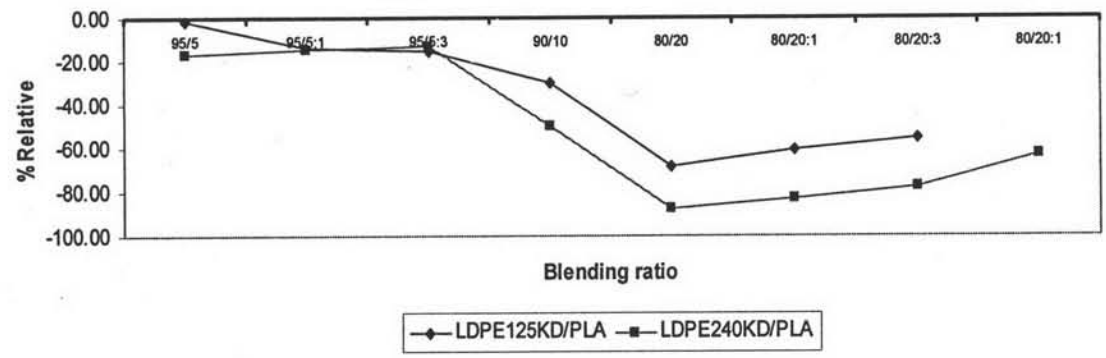

(D) Relative elongation at break

Figure 4.26 Relative mechanical values between LDPE125KD/PLA and LDPE240KD/PLA blend

4.5 Enzymatic degradation study of LDPE/PLA blends

4.5.1 Observation by SEM

The scanning electron micrographs (Figure 27-28) of PLA, LDPE240KD, LDPE125KD and their blends sheets reveal the damaged areas of PLA that is a starting point of the degradation. In SEM micrographs, there are some significant signs in terms of black spots and damaged holes on the PLA surface. The degraded polymer was extracted and then exhibited abnormal holes on LDPE125KD/80 blend surface when compared with LDPE125KD surface. On the other hand, the black spots appeared on LDPE240KD/80 blend surface that might be more difficult to extract the ash from LDPE240KD/80 blend.

SEM photograph illustrates changes in shapes of the porous which are seen black spots of PLA degradation inside LDPE240KD/80:10. Figure 4.27(E) exhibits the reducing effect of the compatibilizer to improve the dispersed phase of PLA (LDPE125KD/80:3) in comparison with that with the compatibilizer as shown in Figure 4.27(D).

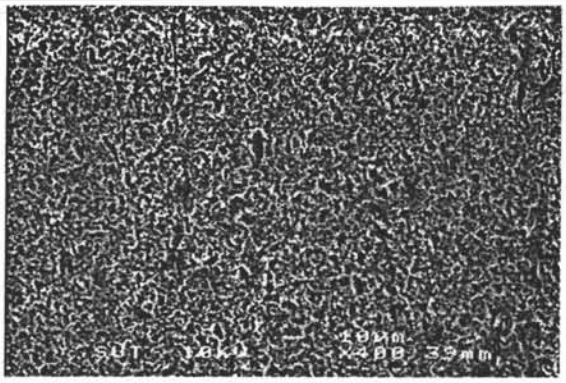

(A) LDPE125KD

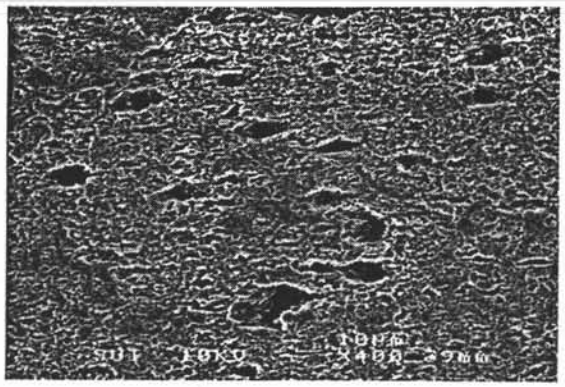

(B) LDPE125KD/80

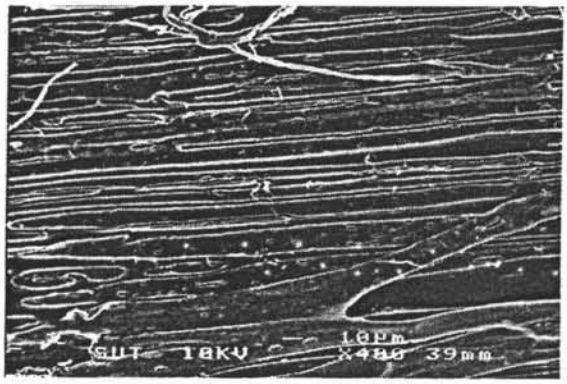

(C) LDPE240KD

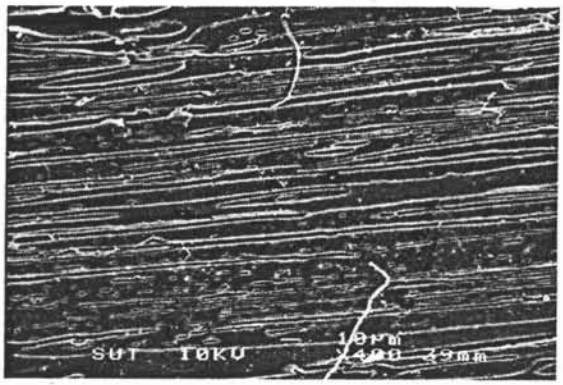

(D) LDPE240KD/80

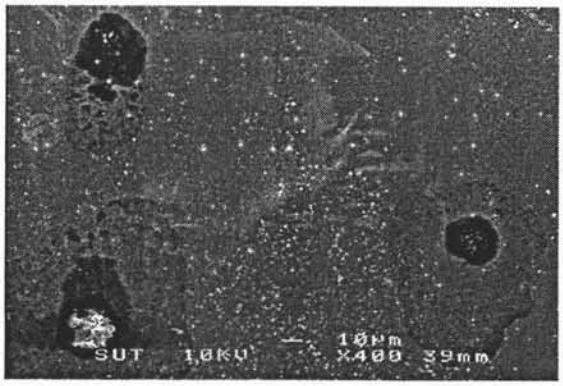

(E) PLA

Figure 4.27 Scanning electron micrographs after 144 hours of enzymatic exposure of: (A) LDPE125KD (B) LDPE125KD/80 blend (C) LDPE240KD (D) LDPE240KD/80 blend and (E) PLA

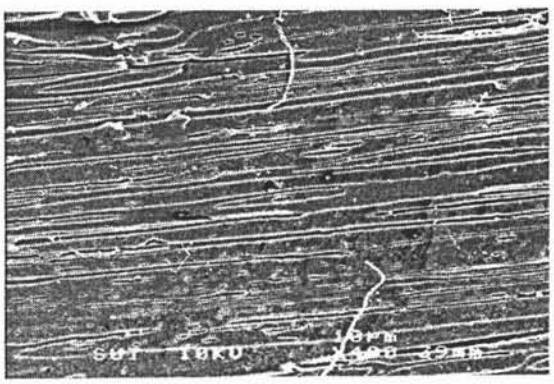

(A) LDPE240KD/80

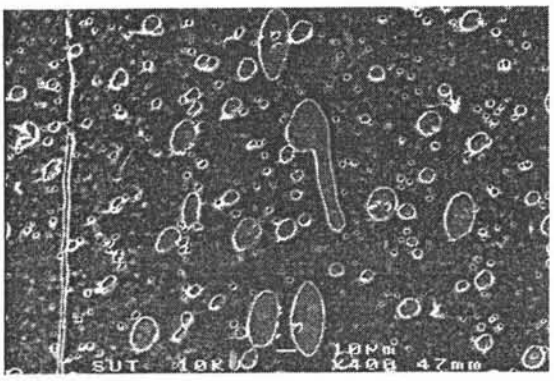

(B) LDPE240KD/80:3

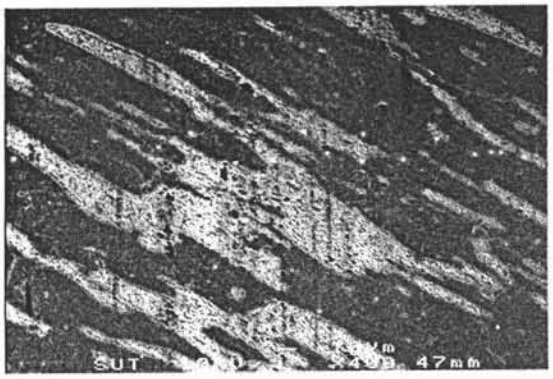

(C) LDPE240KD/80:10

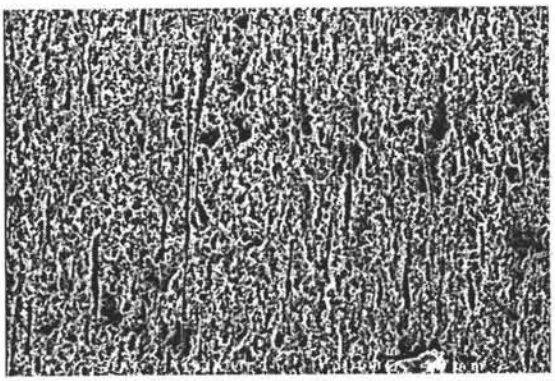

(D) LDPE125KD/80

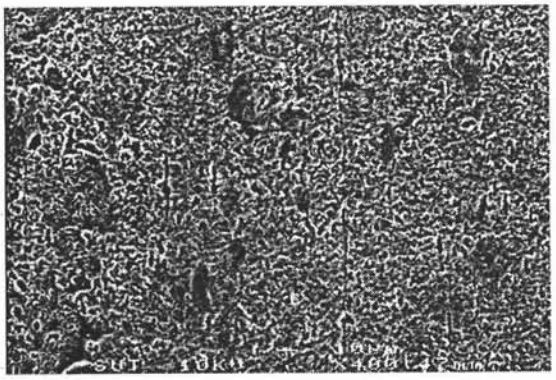

(E) LDPE125KD/80:3

Figure 4.28 Scanning electron micrographs after 144 hours of enzymatic exposure of: the uncompatibilized and compatibilized LDPE240KD/80 and LDPE125KD/80 blends; (A) LDPE240KD/80; (B) LDPE240KD/80:3; (C) LDPE240KD/80:10; (D) LDPE125KD/80; (E) LDPE125KD/80:3

4.5.2 Weight loss investigation

The percentage of weight loss from enzyme degradation show in Figure 4.29 - 4.32. Figure 4.29 illustrates more than 14% weight loss after 144 hours of degradation. The degradation rate of LDPE240KD/80 is higher than that of LDPE125KD/80. This phenomenon can be explained as follows: the PLA size distribution in the LDPE240KD matrix is better than that of the LDPE125KD as shown in Figure 4.3C and 4.3D which gave more contact areas of PLA to the enzyme proteinase K. LLDPE-g-MA help reduce degradation rate is observed in both LDPE240KD and LDPE125KD matrix in which more significant in LDPE240KD indicates by a reducing trend in degradation with increases LLDPE-g-MA amount in LDPE240KD matrix. Hydrolysis reaction of PLA was reduced due to the LLDPE-g-MA coupling with some PLA chains with the LDPE chains.

Basically, LLDPE-g-MA is coupling agent between the PLA and LDPE which causes more difficulties to degrade the compatibilized blends than the uncompatibilized blends. Because the SEM (Figure 4.4 - 4.6) shows a better distribution of PLA in the compatibilized LDPE240KD matrix than LDPE125KD as a result of LLDPE-*g*-MA coupling on PLA chains, the enzymatic degradation of the compatibilized blends is less.

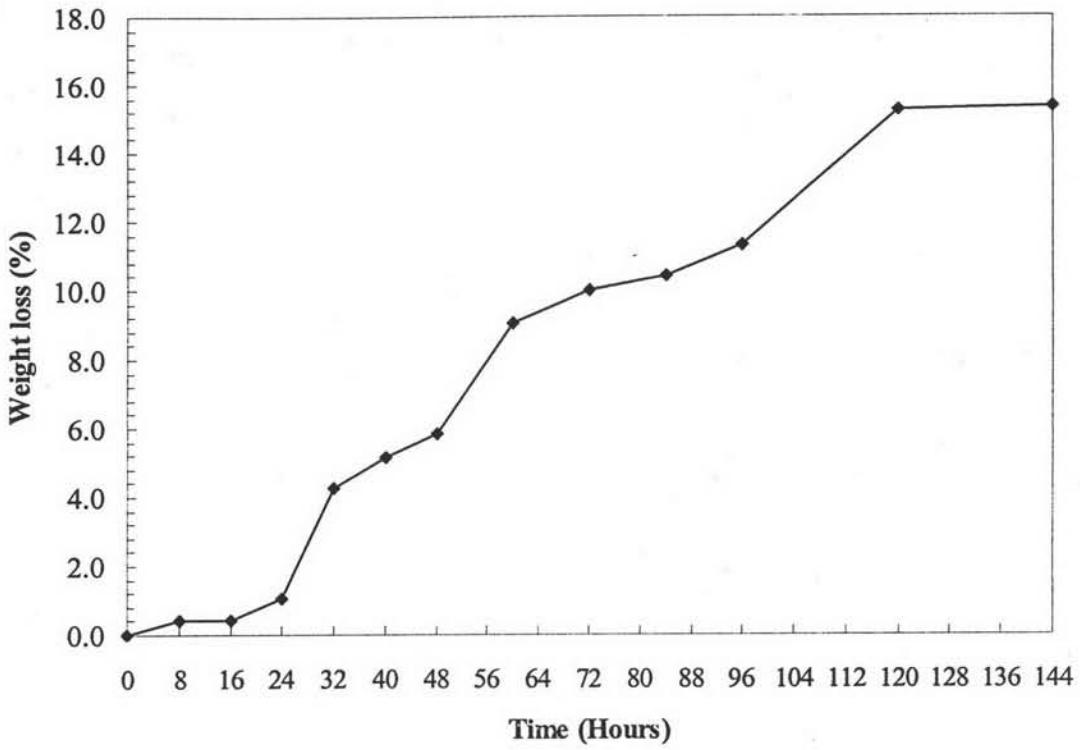

Figure 4.29 Weight loss of PLA on digestion time

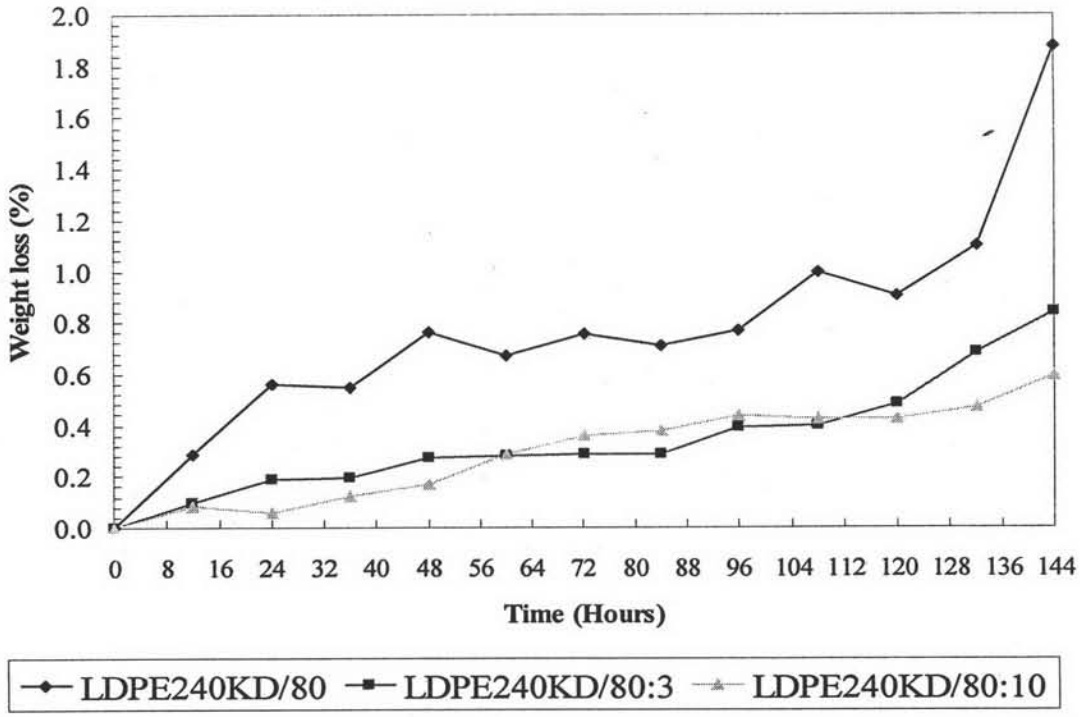

Figure 4.30 Weight loss of the uncompatibilized and compatibilized LDPE240KD/80

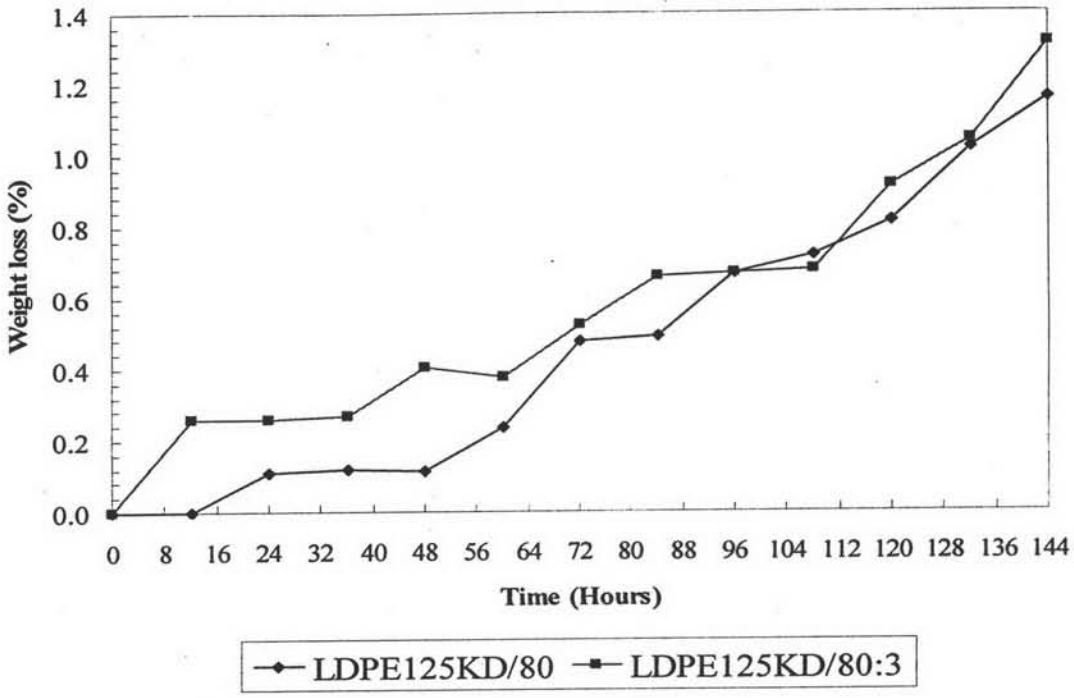

Figure 4.31 Weight loss of the uncompatibilized and compatibilized LDPE125KD/80

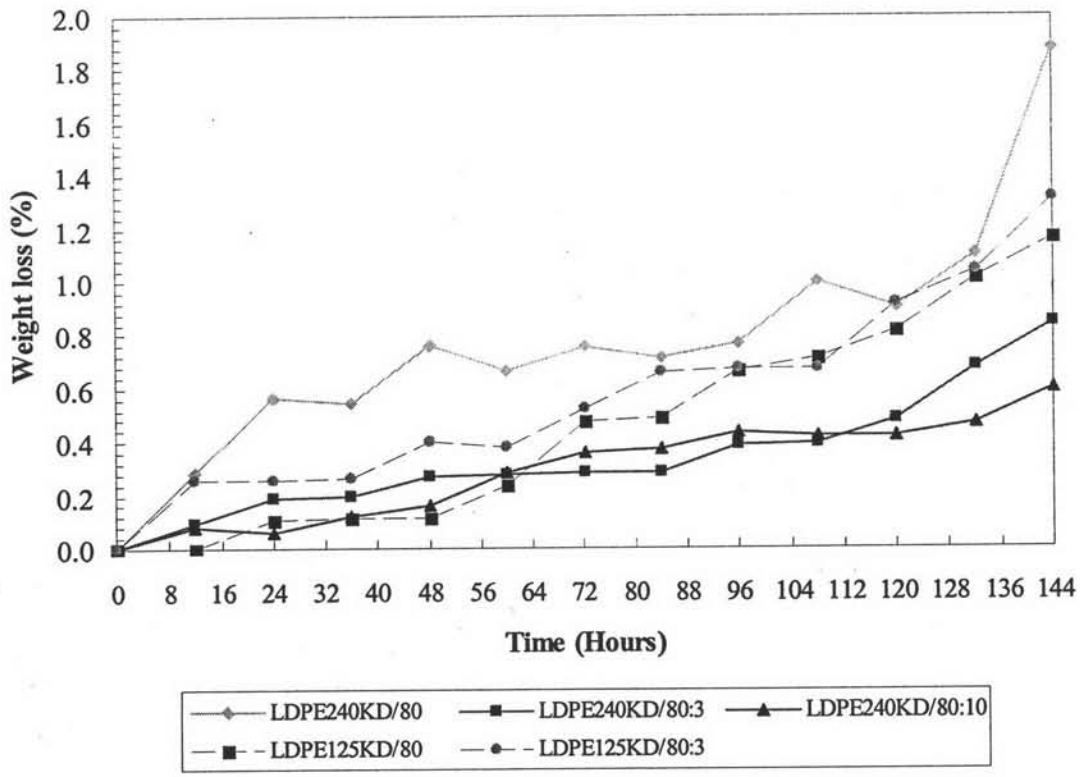

Figure 4.32 Comparison of weight loss between LDPE240KD/80 and LDPE125KD/80